Steel and Composite Structures, *Vol. 31, No. 5 (2019) 469-488*
DOI: https://doi.org/10.12989/scs.2019.31.5.469

Nonlinear bending of functionally graded porous nanobeam subjected to multiple physical load based on nonlocal strain gradient theory

Yang Gao [1a], Wan-shen Xiao [*1] and Haiping Zhu [2a]

[1] *State Key Laboratory of Advanced Design and Manufacturing for Vehicle Body, Hunan University, Changsha, 410082, China*
[2] *School of Computing, Engineering and Mathematics, Western Sydney University, Locked, Bag 1797, Penrith, NSW 2751, Australia*

(*Received November 30, 2018, Revised April 22, 2019, Accepted April 24, 2019*)

Abstract. We in this paper study nonlinear bending of a functionally graded porous nanobeam subjected to multiple physical load based on the nonlocal strain gradient theory. For more reasonable analysis of nanobeams made of porous functionally graded magneto-thermo-electro-elastic materials (PFGMTEEMs), both constituent materials and the porosity appear gradient distribution in the present expression of effective material properties, which is much more suitable to the actual compared with the conventional expression of effective material properties. Besides the displacement function regarding physical neutral surface is introduced to analyze mechanical behaviors of beams made of FGMs. Then we derive nonlinear governing equations of PFGMTEEMs beams using the principle of Hamilton. To obtain analytical solutions, a two-step perturbation method is developed in nonuniform electric field and magnetic field, and then we use it to solve nonlinear equations. Finally, the analytical solutions are utilized to perform a parametric analysis, where the effect of various physical parameters on static bending deformation of nanobeams are studied in detail, such as the nonlocal parameter, strain gradient parameter, the ratio of nonlocal parameter to strain gradient parameter, porosity volume fraction, material volume fraction index, temperature, initial magnetic potentials and external electric potentials.

Keywords: bending; functionally graded porous materials; nonlocal strain graded theory; multiple physical load

1. Introduction

The booming development of industry puts forward higher requirements on material properties so that a variety of composites have been developed and improved by researchers, such as functionally graded materials, sandwich composites, fibre reinforced composite materials, fine grained composites. Among these composite materials, functionally graded materials that were manufactured by Japanese scientists in 1987 have attracted extensive attention in various industries due to its excellent performance (Koizumi 1997). Fig. 1 presents some potential fields for the applications FGMs (Jha *et al*. 2013, Menasria *et al*. 2017, Dai and Dai 2017, Attia *et al*. 2015, Hao 2007, Ma and Lee 2011, Esfahani *et al*. 2013, Dehrouyeh-Semnani 2017, 2018, Wu *et al*. 2016). Thus, functionally graded structures are an advanced class of small-scale structures with promising applications in nanotechnology and microtechnology (Ghayesh and Farajpour 2019). Specifically speaking, functionally graded materials in which the composition and structure show continuous gradient change can satisfy the requirements of the functional and performance change with position on design of each component. In terms of such concept, functionally graded pizezomagntic and piezoelectric materials were designed intentionally to acquire more pronounced magneto-electric coupling effect, the results of which have captured plenty of attention in engineering applications as well as scientific researches (Saadatfar and Aghaie-Khafri 2014, Ke *et al*. 2012, Hamidi *et al*. 2015, Guo and Wang 2017). For instance, Arani *et al*. (2010) used the material to extend the availability of life span of intelligent equipment. Consequently, researches relevant to functionally graded magnetic-electric-elastic materials were, are and remain to be a hot topic.

Based on the special structure of FGMs, those classical theories, like Reddy beam model, Timoshenko beam model and Euler-Bernoulli beam model, should be modified in analyzing problems of FGMs. So far, a multitude of researches related to FGMs have been performed by using those modified methods and modified displacement fields. Eltaher *et al*. (2013) proposed a modified functionally graded beam theory to determine neutral axis position, then to study its effect on line vibration of nanobeams. More importantly, Zhang and Fu (2013) for the first time derived a high order shear deformation theory including the physical neutral surface, which is a groundbreaking study regarding the displacement functions of functionally graded materials. Subsequently, the high order shear deformation theory were employed to investigate the nonlinear bending behaviors of FGM beams (Zhang 2013) and nonlinear bending behaviors of FGM infinite cylindrical shallow shells (Zhang 2015) where the results obtained by Ritz method revealed the major difference between components made of FGMs and components made of homogeneous materials. Therefore, it is necessary to introduce the theory

∗Corresponding author, Professor,
E-mail: xwshndc@126.com

http://www.techno-press.org/?journal=scs&subpage=6 ISSN: 1229-9367 (Print), 1598-6233 (Online)

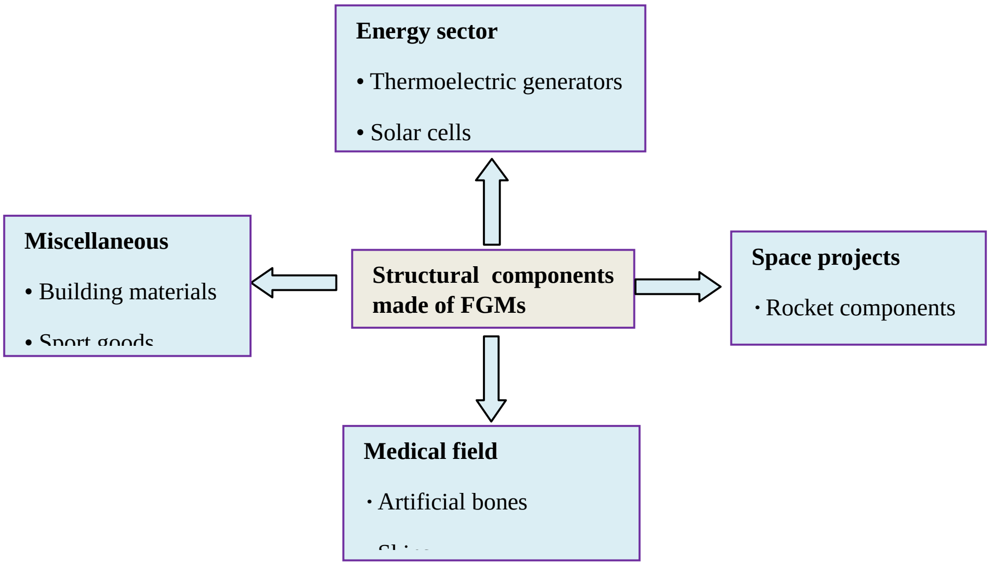

Fig. 1 Potential fields for the applications FGMs

to deal with problems of FGMs throughout the course of our study.

Moreover owing to porosity appearing in functionally graded materials during manufacturing production, it is reasonable to take into account for influence of porosity on mechanical behaviors of structures. Chen *et al*. (2015) studied critical buckling load and static bending deformation of functionally graded beams subjected to two porosity distribution patterns. Chen *et al*. (2016) provided a possible approach to improve the nonlinear vibration behaviors of porous beams through comparing different types of porosity distribution. Sahmani *et al*. (2018) explored the size-dependent in nonlinear vibration response of FG porous plates, for which the model of the Halpin-Tsai micromechanical and a simple perturbation method were used to undertake the research. Except for above-mentioned studies on FG porous beams, the team led by She respectively investigated buckling and post-buckling behaviors of FG porous tubes (She *et al*. 2017), linear vibrations of FG porous tubes (She *et al*. 2018a) as well as wave propagation of FG porous tubes (She *et al*. 2018b) with the aid of a refined beam model. However, to authors' knowledge, there is no static analysis of porous beams made of functionally graded magnetic -thermo-electric-elastic materials. So, it is worthwhile to take much effort and some time to make clear of the mechanical properties for PFGMTEEMs beams.

When analyzing the problems involving nano-structures, the effect of size-dependent on the mechanical behaviors can not be ignored, which has been demonstrated by the experimental results, such as experimental evaluation of the length scale for nanocantilevers (Tang and Alici 2011a, b), experimental evaluation of positive size effects for the bending of micromaterials (Liebold and Müller 2016) and experimental study of size-dependent vibration for nickel cantilever microbeams (Lei *at al*. 2016). Nevertheless, the classical theories are unable to characterize the size effect in nano-structures, because of lack of additional length scale parameters. To overcome the difficulty, some researchers had to put forward novel non-classical continuum models to capture the size effect, such as nonlocal elasticity theory, strain gradient theory and nonlocal strain gradient theory. The nonlocal elasticity theory proposed by Eringen and Edelen (1972) assumes that the stress tensor at a given point is not only dependent on the strain at the reference point but also dependent on the strains at all points in the total body. Later, a series of researches with respect to nano-structures have been carried out in recent years, which manifest that the stiffness-softening effect can be taken into account via the theory (Nejad *et al*. 2016, Barati 2017, Ghadiri *et al*. 2017, Rahmani and Pedram 2014, Thai *et al*. 2018). The strain gradient theory proposed by Mindlin (1965) that includes sixteen additional higher order material constants is another size-dependent non-classical theory. Such theory states that additional strain graded terms should be incorporated into the total stress field in analysis of mechanism of nano-structures. Afterwards, Lam *et al*. (2003) developed a modified strain gradient theory where the number of the non-classical material parameters is reduced to three, whereas determining the values of non-classical material length scale parameters is still fraught with difficulties. Consequently, the modified couple stress theory (MCST) elaborated by Yang *et al*. (2002), including merely one non-classical material length scale parameter as well as double classical ones, assumes that the strain energy density is determined by the strain tensor aligned with the symmetric part of the curvature tensor, which can be regarded as the special case of the modified strain gradient theory. In terms of these modified theories, a number of relevant studies have been performed (Dehrouyeh-Semnani and Bahrami 2016, Simsek and Reddy 2013, Fourn *et al*. 2018, Abdelaziz *et al*. 2017, Dehrouyeh-Semnani *et al*. 2015, 2016, 2017, Chen *et al*. 2019, Bhattacharya and Debabrata 2019, Ghayesh *et al*. 2017), indicating that the stiffness-hardening effect can be taken into account via the theories. To consider two types of size-dependent effect, the stiffness-softening effect and the stiffness-hardening effect, in the same theoretical frame-work, Lim *et al*. (2015) put forward the nonlocal strain gradient theory that reasonably builds a bridge between nonlocal elasticity theory and strain gradient theory. But the computational costs of the theory is larger than those of the nonlocal elasticity theory and strain gradient theories, because both the nonlocal term and stain gradient term are taken into account (Farajpour *et al*. 2018). Based on the excellent theory, nonlinear vibration of functionally graded nanobeams (Şimşek 2016, Lu *et al*. 2017, Li *et al*. 2016a, Ebrahimi and Barati 2017, Liu *et al*. 2019, She *et al*. 2018c), longitudinal vibration of size-dependent rods (Li *et al*. 2016b, El-Borgi *et al*. 2018), nonlinear vibration of nanotubes (Ghayesh and Farajpour 2018a, She *et al*. 2018d, Ghayesh and Farajpour 2018b, Farajpour et al. 2019), nonlinear bending of curved nanotubes(She *et al*. 2019) and linear bending, buckling and vibration of FG nanobeams (Li *et al*. 2017) were studied in the past, the results of which revealed the relation between nonlocal parameters and strain gradient parameters very fully.

Even though the nonlocal strain gradient theory has been widely used to study mechanical behaviors of nano-materials, there are a few papers regarding nano-structures made of functionally graded magneto-thermo- electric-elastic materials in the open literature. Ebrahimi and Dabbagh (2017a) used the theory to perform an exact investigation of wave propagation in smart rotating magneto-electro-elastic nanoplates. Ma *et al*. (2017) studied wave propagation in MEE shells using the theory whose research focus is the influence of nonlocal parameter and length scale parameter on wave propagation. A higher-order shear deformation in conjunction with the theory were used to induce the nonlocal governing equations by Ebrahimi and Dabbagh (2017b), where electric voltages, wave number, magnetic potential, nonlocal parameter and length scale parameter were analyzed in detail. Ebrahimi and Barati (2016a) developed a nonlocal strain gradient beam model, then used it to study natural frequencies of axially functionally graded beams subjected to a nonuniform magnetic field. From this review of the literature, we have a good knowledge that there is no study relevant to nonlinear bending of functionally graded magneto-thermo-electro-elastic nanobeams. So, it is worth doing it.

Obtaining analytical solutions from governing equations is always a tough task, especially for solving nonlinear equations. To overcome this difficulty, researchers proposed and developed various methods for resolving nonlinear equations, such as perturbation methods (Mook and Nayfeh 1979), harmonic balance method (Dai *et al*. 2014), differential transformation method (Zhou 1986) and high dimensional harmonic balance method (Hall *et al*. 2015). Among these methods, perturbation methods have been widely applied into scientific researches due to their simple and practical significance. For instance, a two-step perturbation method as one of perturbation methods was utilized to study nonlinear vibration of tubes by Zhong *et al*. (2016). Then, with the aid of their analytical solutions, buckling and post-buckling behaviors of nanotubes was studied by She *et al*. (2017) and nonlinear vibration of functionally graded porous nanoplates was studied by Sahmani *et al*. (2018). Differing from previous studies, authors in this article attempt to introduce a two-step perturbation method into nonuniform electric field and magnetic field, the purpose of which is to obtain analytical solutions, and then to get a sense for usage.

Our study is motivated via the recent analysis of the strain gradient length scale, the nonlocal parameters and so on within the theoretical framework of the nonlocal strain gradient theory. Firstly, the porosity distribution and material distribution along the thickness are taken into account in the present effective material properties of porous functionally graded magneto-thermo-electro-elastic materials. Secondly, the displacement function regarding the physical neutral surface is used to study mechanical behaviors of beams made of FGMs. Thirdly, within the theoretical framework of the nonlocal strain gradient theory, analytical solutions obtained by an improved perturbation method are used to analyze the influence of respective physical parameters on the static bending deformation of PFGMTEEMs nanobeams.

2. Basic equations

2.1 Nonlocal strain gradient theory

Differing from the Eringen's nonlocal theory (Eringen and Edelen 1972) stating that the stress tensor at a given point is not only dependent on the strain at the reference point but, more importantly, dependent on the strains at all points in the entire body and the strain gradient theory (Thai *et al*. 2018, Yang *et al*. 2002) stating that the physical material properties should be considered as atoms associated with the higher-order deformations on the nanometer length rather than merely modeled them as a collection of points, the nonlocal strain gradient theory proposed by Lim *et al*. (2015) takes into account for effects of the nonlocal elastic stress field and the strain gradient stress field in the whole stress field. Consequently, via introducing two scale parameters, the theory can be expressed as for magneto-thermo-electric-elastic solids (Ma *et al*. 2017)

$$[1-(e_0a)^2\nabla^2]\sigma_{ij} = \left(1-l^2\nabla^2\right)\left[c_{ijkl}\varepsilon_{kl}\left(x'\right) - e_{mij}E_m(x') - q_{nij}H_n(x') - c_{ijkl}\alpha_{kl}\Delta T\right] \quad (1)$$

$$[1-(e_0a)^2\nabla^2]D_i = \left(1-l^2\nabla^2\right)\left[e_{ikl}\varepsilon_{kl}\left(x'\right) + s_{im}E_m(x') + d_{in}H_n(x') - p_i\Delta T\right] \quad (2)$$

$$[1-(e_0a)^2\nabla^2]B_i = \left(1-l^2\nabla^2\right)\left[q_{ikl}\varepsilon_{kl}\left(x'\right) + d_{im}E_m(x') + \chi_{in}H_n(x') - \lambda_i\Delta T\right] \quad (3)$$

$$D_{i,i} = 0; B_{i,i} = 0; \quad (4)$$

$$\varepsilon_{ij} = \frac{1}{2}(u_{i,j} + u_{j,i}); E_i = -\phi_{E,i}; H_i = -\varphi_{H,i}; \quad (5)$$

where σ_{ij}, ε_{ij}, D_i, E_i, B_i, and H_i respectively stand for the stress, strain, electric displacement, electric field, magnetic induction as well as magnetic field; c_{ijkl}, e_{mij}, s_{im}, q_{nij}, d_{in}, χ_{in}, p_i, λ_i, α_{kl}, ΔT, Φ, φ and u_i are elastic, piezoelectric, dielectric piezomagnetic, magnetoelectric, magnetic permeability coefficient, pyroelectric constants, pyromagnetic constants,

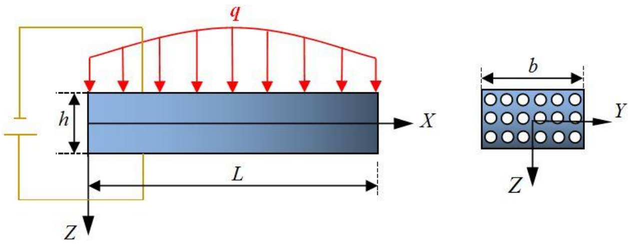

Fig. 2 Schematic configuration of a beam made of PFGMTEEMs

the thermal expansion coefficient, temperature change, electric potential, magnetic potential and displacement components, separately; Both the nonlocal parameter e_0a and the length scale parameter l are used to account for the size-dependent effect of nanostructures; ∇^2 is the Laplace operator.

We can infer that the nonlocal elasticity constitutive equations can be obtained from the above differential constitutive Eqs. (1)-(3) when setting l equal to zero and the strain gradient constitutive equations can be obtained from the above differential constitutive Eqs. (1)-(3) when setting e_0a equal to zero. Obviously, the nonlocal strain gradient theory can build a bridge between the Eringen's nonlocal theory and the strain gradient theory, thus making it possible to more reasonably characterize the size-dependent effect.

2.2 Description of the structure

For a beam made of porous functionally graded magneto-thermos-electric-elastic materials, the effective material properties can be defined as (Xiao *et al*. 2018)

$$P_f = P(z)\left(1-\frac{\gamma}{2}\right) \text{ and } P(z) = (P_2 - P_1)\left(\frac{z}{h}+\frac{1}{2}\right)^N + P_1 \quad (6)$$

Here, P_1 and P_2 respectively represent the physical material properties of $BaTiO_3$ and $CoFeO_4$. Combined with Fig. 2, we have a good knowledge that the top surface at $z = -h/2$ is full of $BaTiO_3$, while the bottom surface $z = +h/2$ is full of $CoFeO_4$. Moreover, the symbols of N and γ are the volume fraction index ($0 \le N < \infty$) and porosity volume fraction ($0 \le \gamma < 1$). In this article, we merely study the beams subjected to evenly distributed porosity.

It is indicated from Eq. (6) that the porosity and material properties are simultaneously distributed along the thickness of the beam in the present even porosity distribution.

$$P_f = (P_2 - P_1)\left(\frac{z}{h}+\frac{1}{2}\right)^N + P_1 - \frac{\gamma\left(P_1 + P_2\right)}{2} \quad (7)$$

From the perspective of common fabrication methods of FGMs, as presented in Table 1, the present is much more suitable to the actual porosity distribution compared with the conventional even porosity distribution shown in Eq. (7). The reason is that a porous beam has porosities

Table 1 Common fabrication methods of functionally graded materials (Miyamoto *et al*. 2001, Kieback *et al*. 2003, Tao *et al*. 2012)

Fabrication methods		**Main features**
Powder metallurgy method	Powder accumulation	• Production process is simple. • Distribution of components are discontinuous. • Number of accumulation layer is limited. • Production efficiency is low. • Only be suitable for experiments.
	Wet powder spraying	• Distribution of components are continuous. • Control accuracy is high. • Thickness of accumulation layer is small.
	Slip casting	• Distribution of components are continuous. • Be very suitable for batch production.
Centrifugal casting method		• Production process and equipment are simple. • Production efficiency is high and cost is low. • Conventional raw materials can be used. • Can produce large FGMs with high compactness.
Electro-deposition method		• Production equipment is simple and cost is low. • Damage to the matrix material is small. • Be very suitable for thin-walled box FGMs.
Laser cladding method		• Can be used on matrix with arbitrary curved surface. • Control accuracy is high and preparation time is short. • Production equipment are complex and expensive.
Vapor deposition method	Physical vapor deposition	• Deposition is fast, controls of components are accurate, and bond strength is high. • Only be suitable for FGMs with small sizes.
	Chemical vapor deposition	• Temperature effect is small. • Deposition is slow, controls of components are discontinuous, and bond strength is high. • FGMs has low compactness and low bond strength.
Plasma spraying method		• Be very suitable for ceramic/metal FGMs with large sizes. • Be easy to control, cost is moderate. • Porosity is high, and bond strength is low

spreading through the thickness due to defect during production, which is a random process.

3. Nonlinear PFGMTEEMs beam model

As vividly illustrated in Fig. 2, a porous beam with length L, width b and thickness h is subjected to an electric potential Φ, a magnetic potential φ, two kinds of transverse load q as well as a uniform temperature field T. A Cartesian coordinate system (O, X, Y, Z) is set at the geometric middle plane of the beam where the axis of X coincides with symmetric axis of this beam and the axis of Z is perpendicular to O-XY plane. Based on the high order shear deformation theory (Zhang 2013), the displacement functions can be expressed as

$$\begin{aligned} u_1(x,y,z) &= u_0(x) + (z - z_0)\theta - c_1\left(z^3 - c_0\right)\left(\frac{\mathrm{d}w}{\mathrm{d}x} + \theta\right) \\ u_2(x,y,z) &= 0 \\ u_3(x,y,z) &= w(x) \end{aligned} \tag{8}$$

where u_0 and $w(x)$ are respective displacements in the direction of X axis and Z axis, and θ stands for rotation angle with respective to the physical neutral axis. Here, z_0 and c_0 are respectively given by

$$z_0 = \frac{\int_A zE(z,T)\,\mathrm{d}\sigma}{\int_A E(z,T)\,\mathrm{d}\sigma};\quad c_0 = \frac{\int_A z^3E(z,T)\,\mathrm{d}\sigma}{\int_A E(z,T)\,\mathrm{d}\sigma}$$

It should be mentioned out that the physical neutral surface determined by z_0 is changed with variational temperature, partly because the effective material properties are assumed to be temperature-dependent. As a result, the physical neutral surface does not coincide with the geometric middle plane of this beam unless for beams made of isotropic materials, both z_0 and c_0 are equivalent to zero.

With the aid of von-karman nonlinear strain displacements theory, the correlation between nonlinear strains and displacements can be arrived at

$$\varepsilon_{xx} = \frac{\partial u_1}{\partial x} + \frac{1}{2}\left(\frac{\mathrm{d}u_3}{\mathrm{d}x}\right)^2 = \varepsilon_x^{(0)} + (z - z_0)\varepsilon_x^{(1)} - c_1\left(z^3 - c_0\right)\varepsilon_x^{(3)};\ \gamma_{xz} = \frac{\mathrm{d}u_3}{\mathrm{d}x} + \frac{\mathrm{d}u_1}{\mathrm{d}z} = \gamma_{xz}^{(0)} - c_2 z^2 \gamma_{xz}^{(2)} \tag{9}$$

where

$$\varepsilon_x^{(0)} = \frac{\mathrm{d}u_0}{\mathrm{d}x} + \frac{1}{2}\left(\frac{\mathrm{d}w}{\mathrm{d}x}\right)^2;\ \varepsilon_x^{(1)} = \frac{\mathrm{d}\theta}{\mathrm{d}x};\ \varepsilon_x^{(3)} = \frac{\mathrm{d}\theta}{\mathrm{d}x} + \frac{\mathrm{d}^2 w}{\mathrm{d}x^2};\ \gamma_{xz}^{(0)} = \gamma_{xz}^{(2)} = \theta + \frac{\mathrm{d}w}{\mathrm{d}x};\ c_1 = \frac{4}{3h^2};\ c_2 = \frac{4}{h^2};$$

In this study, the distributions of electric potentials and magnetic potentials are supposed to be a combination of linear and cosine variations (Ansari *et al*. 2015)

$$\phi_E(x,z,t) = -\cos(\beta z)\phi(x,t) + \frac{2zV_0}{h} \tag{10}$$

$$\varphi_H(x,z,t) = -\cos(\beta z)\varphi(x,t) + \frac{2z\Omega}{h} \tag{11}$$

where $\beta = \pi/h$, V_0 and Ω shown in Eqs. (10)-(11) respectively stand for the applied initial external electric voltage and magnetic potential. The components of the electric fields (E_x, E_z) and magnetic fields (H_x ,H_z) can be derived via substituting Eqs. (10)-(11) into Eq. (5).

$$E_x = -\frac{\partial \phi_E}{\partial x} = \cos(\beta z)\frac{\partial \phi}{\partial x} \tag{12}$$

$$E_z = -\frac{\partial \phi_E}{\partial z} = -\beta\sin(\beta z)\phi(x,t) - \frac{2V_0}{h} \tag{13}$$

$$H_x = -\frac{\partial \varphi_H}{\partial x} = \cos(\beta z)\frac{\partial \varphi}{\partial x} \tag{14}$$

$$H_z = -\frac{\partial \varphi_H}{\partial z} = -\beta\sin(\beta z)\varphi(x,t) - \frac{2\Omega}{h} \tag{15}$$

According to the Hamilton's principle, we have

$$\int_0^t \left(\delta\Pi_S + \delta\Pi_W\right) = 0 \tag{16}$$

where Π_S is the strain energy and Π_W is the work performed by external forces.

The variation of the virtual strain energy is given by

$$\delta\Pi_S = \int_0^L \int_{-h/2}^{h/2} (\sigma_{xx}\delta\varepsilon_{xx} + \sigma_{xz}\delta\gamma_{xz} - D_x\delta E_x - D_z\delta E_z - B_x\delta H_x - B_z\delta H_z)\,\mathrm{d}x\mathrm{d}z \tag{17}$$

We substitute Eqs. (9) and (12)-(15) into Eq. (17), obtaining

$$\begin{aligned} \delta\Pi_S = {} & \int_0^L [N\delta\varepsilon_x^{(0)} + M\delta\varepsilon_x^{(1)} - c_1 P\delta\varepsilon_x^{(3)} + (Q - c_2 R)\delta\gamma_{xz}^{(0)}]\mathrm{d}x - \int_0^L\int_A \left\{D_x\cos(\beta z)\delta\frac{\partial\phi}{\partial x} - D_z\beta\sin(\beta z)\delta\phi\right\}\mathrm{d}A\mathrm{d}x \\ & - \int_0^L\int_A \left\{B_x\cos(\beta z)\delta\frac{\partial\varphi}{\partial x} - B_z\beta\sin(\beta z)\delta\varphi\right\}\mathrm{d}A\mathrm{d}x \end{aligned} \tag{18}$$

in which

$$(N,M,P) = \int_{-h/2}^{h/2}\int_{-h/2}^{h/2}\left[\sigma_{xx}, \sigma_{xx}(z - z_0), \sigma_{xx}(z^3 - c_0)\right]\mathrm{d}z\mathrm{d}y;\ (Q,R) = \int_{-h/2}^{h/2}\int_{-h/2}^{h/2}(\sigma_{xz}, \sigma_{xz}z^2)\mathrm{d}z\mathrm{d}y;$$

The variation of the work produced by the external force is written as

$$\delta\Pi_W = -\int_0^L q\delta w\mathrm{d}x - \int_0^L (N_E + N_H + N_T)\frac{\mathrm{d}w}{\mathrm{d}x}\delta\left(\frac{\mathrm{d}w}{\mathrm{d}x}\right)\mathrm{d}x \tag{19}$$

where N_E, N_H and N_T represent the normal forces produced by external electrical potential V_0, magnetic potential Ω and uniform temperature rise ΔT, respectively.

$$N_E = -\int_{-h/2}^{h/2}\frac{2e_{31}V_0}{h}\mathrm{d}z;\ N_H = -\int_{-h/2}^{h/2}\frac{2q_{31}\Omega}{h}\mathrm{d}z;\ N_T = \int_{-h/2}^{h/2} c_{11}\alpha_f(T - T_0)\mathrm{d}z;$$

For one-dimension beam, the nonlocal strain graded constitutive Eqs. (1)-(3) can be achieved as

$$\sigma_{xx} - \mu^2\frac{\mathrm{d}^2\sigma_{xx}}{\mathrm{d}x^2} = \left(1 - l^2\nabla^2\right)\left\{\begin{aligned} & c_{11}\left[\frac{\mathrm{d}u_0}{\mathrm{d}x} + \frac{1}{2}\left(\frac{\mathrm{d}w}{\mathrm{d}x}\right)^2 + (z - z_0)\frac{\mathrm{d}\theta}{\mathrm{d}x} - c_1\left(z^3 - c_0\right)\left(\frac{\mathrm{d}\theta}{\mathrm{d}x} + \frac{\mathrm{d}^2 w}{\mathrm{d}x^2}\right)\right] \\ & + e_{31}\left[\beta\sin(\beta z)\phi + \frac{2V_0}{h}\right] + q_{31}\left[\beta\sin(\beta z)\varphi + \frac{2\Omega}{h}\right] - c_{11}\alpha_f\Delta T \end{aligned}\right\} \tag{20}$$

$$\sigma_{xz} - \mu^2\frac{\mathrm{d}^2\sigma_{xz}}{\mathrm{d}x^2} = \left(1 - l^2\nabla^2\right)\left[c_{55}(1 - c_2 z^2)\left(\theta + \frac{\mathrm{d}w}{\mathrm{d}x}\right) - e_{15}\cos(\beta z)\frac{\mathrm{d}\phi}{\mathrm{d}x} - q_{15}\cos(\beta z)\frac{\mathrm{d}\varphi}{\mathrm{d}x}\right] \tag{21}$$

$$D_x-\mu^2\frac{\mathrm{d}^2D_x}{\mathrm{d}x^2}=\left(1-l^2\nabla^2\right)\left[e_{15}(1-c_2z^2)\left(\theta+\frac{\mathrm{d}w}{\mathrm{d}x}\right)+s_{11}\cos(\beta z)\frac{\mathrm{d}\phi}{\mathrm{d}x}+d_{11}\cos(\beta z)\frac{\mathrm{d}\varphi}{\mathrm{d}x}\right] \tag{22}$$

$$D_z-\mu^2\frac{\mathrm{d}^2D_x}{\mathrm{d}x^2}=\left(1-l^2\nabla^2\right)\left\{\begin{array}{l}e_{31}\left[\frac{\mathrm{d}u_0}{\mathrm{d}x}+\frac{1}{2}\left(\frac{\mathrm{d}w}{\mathrm{d}x}\right)^2+\left(z-z_0\right)\frac{\mathrm{d}\theta}{\mathrm{d}x}-c_1\left(z^3-c_0\right)\left(\frac{\mathrm{d}\theta}{\mathrm{d}x}+\frac{\mathrm{d}^2w}{\mathrm{d}x^2}\right)\right]\\ -s_{33}\left[\beta\sin(\beta z)\phi+\frac{2V_0}{h}\right]-d_{33}\left(\beta\sin(\beta z)\varphi+\frac{2\Omega}{h}\right)+p_3\Delta T\end{array}\right\} \tag{23}$$

$$B_x-\mu^2\frac{\mathrm{d}^2B_x}{\mathrm{d}x^2}=\left(1-l^2\nabla^2\right)\left[q_{15}(1-c_2z^2)\left(\theta+\frac{\mathrm{d}w}{\mathrm{d}x}\right)+d_{11}\cos(\beta z)\frac{\mathrm{d}\phi}{\mathrm{d}x}+\chi_{11}\cos(\beta z)\frac{\mathrm{d}\varphi}{\mathrm{d}x}\right] \tag{24}$$

$$B_z-\mu^2\frac{\mathrm{d}^2B_z}{\mathrm{d}x^2}=\left(1-l^2\nabla^2\right)\left\{\begin{array}{l}q_{31}\left[\frac{\mathrm{d}u_0}{\mathrm{d}x}+\frac{1}{2}\left(\frac{\mathrm{d}w}{\mathrm{d}x}\right)^2+\left(z-z_0\right)\frac{\mathrm{d}\theta}{\mathrm{d}x}-c_1\left(z^3-c_0\right)\left(\frac{\mathrm{d}\theta}{\mathrm{d}x}+\frac{\mathrm{d}^2w}{\mathrm{d}x^2}\right)\right]\\ -d_{33}\left[\beta\sin(\beta z)\phi+\frac{2V_0}{h}\right]-\chi_{33}\left(\beta\sin(\beta z)\varphi+\frac{2\Omega}{h}\right)+\lambda_3\Delta T\end{array}\right\} \tag{25}$$

After substituting Eqs. (18)-(19) into Eq. (16), and setting the coefficients of δu, $\delta\theta$, δw, $\delta\Phi$, $\delta\varphi$ to zero, we can obtain the nonlinear governing equations of the beam.

$$\delta u:\frac{\mathrm{d}N}{\mathrm{d}x}=0 \tag{26}$$

$$\delta\theta:\frac{\mathrm{d}M}{\mathrm{d}x}-c_1\frac{\mathrm{d}P}{\mathrm{d}x}-Q+c_2R=0 \tag{27}$$

$$\delta w:N\frac{\mathrm{d}^2w}{\mathrm{d}x^2}+c_1\frac{\mathrm{d}^2P}{\mathrm{d}x^2}+\frac{\mathrm{d}Q}{\mathrm{d}x}-c_2\frac{\mathrm{d}R}{\mathrm{d}x}+q-(N_E+N_H+N_T)\frac{\mathrm{d}^2w}{\mathrm{d}x^2}=0 \tag{28}$$

$$\delta\phi:\int_A\left[\frac{\mathrm{d}D_x}{\mathrm{d}x}\cos(\beta z)+D_z\beta\sin(\beta z)\right]\mathrm{d}A=0 \tag{29}$$

$$\delta\varphi:\int_A\left[\frac{\mathrm{d}B_x}{\mathrm{d}x}\cos(\beta z)+B_z\beta\sin(\beta z)\right]\mathrm{d}A=0 \tag{30}$$

In terms of the nonlocal strain graded constitutive Eqs. (20)-(25), the stress resultants of PFGMTEEMs beam are determined as

$$N-\mu^2\frac{\mathrm{d}^2N}{\mathrm{d}x^2}=\left(1-l^2\nabla^2\right)\left[\frac{A_{11}}{2}\left(\frac{\mathrm{d}w}{\mathrm{d}x}\right)^2+B_{11}\frac{\mathrm{d}\theta}{\mathrm{d}x}-c_1E_{11}\left(\frac{\mathrm{d}\theta}{\mathrm{d}x}+\frac{\mathrm{d}^2w}{\mathrm{d}x^2}\right)-N_E-N_H-N_T\right] \tag{31}$$

$$M-\mu^2\frac{\mathrm{d}^2M}{\mathrm{d}x^2}=\left(1-l^2\nabla^2\right)\left[\frac{B_{11}}{2}\left(\frac{\mathrm{d}w}{\mathrm{d}x}\right)^2+D_{11}\frac{\mathrm{d}\theta}{\mathrm{d}x}-c_1F_{11}\left(\frac{\mathrm{d}\theta}{\mathrm{d}x}+\frac{\mathrm{d}^2w}{\mathrm{d}x^2}\right)+E_{31}\phi+Q_{31}\varphi-M_E-M_H-M_T\right] \tag{32}$$

$$P-\mu^2\frac{\mathrm{d}^2P}{\mathrm{d}x^2}=\left(1-l^2\nabla^2\right)\left[\frac{E_{11}}{2}\left(\frac{\mathrm{d}w}{\mathrm{d}x}\right)^2+F_{11}\frac{\mathrm{d}\theta}{\mathrm{d}x}-c_1H_{11}\left(\frac{\mathrm{d}\theta}{\mathrm{d}x}+\frac{\mathrm{d}^2w}{\mathrm{d}x^2}\right)+F_{31}\phi+G_{31}\varphi-P_E-P_H-P_T\right] \tag{33}$$

$$Q-\mu^2\frac{\mathrm{d}^2Q}{\mathrm{d}x^2}=\left(1-l^2\nabla^2\right)\left[(A_{55}-c_2D_{55})\left(\theta+\frac{\mathrm{d}w}{\mathrm{d}x}\right)-E_{15}\frac{\mathrm{d}\phi}{\mathrm{d}x}-Q_{15}\frac{\mathrm{d}\varphi}{\mathrm{d}x}\right] \tag{34}$$

$$R-\mu^2\frac{\mathrm{d}^2R}{\mathrm{d}x^2}=\left(1-l^2\nabla^2\right)\left[(D_{55}-c_2F_{55})\left(\theta+\frac{\mathrm{d}w}{\mathrm{d}x}\right)-F_{15}\frac{\mathrm{d}\phi}{\mathrm{d}x}-G_{15}\frac{\mathrm{d}\varphi}{\mathrm{d}x}\right] \tag{35}$$

$$\int_A\left(D_x-\mu^2\frac{\mathrm{d}^2D_x}{\mathrm{d}x^2}\right)\cos(\beta z)\mathrm{d}A=\left(1-l^2\nabla^2\right)\left[(E_{15}-c_2F_{15})\left(\theta+\frac{\mathrm{d}w}{\mathrm{d}x}\right)+X_{11}\frac{\mathrm{d}\phi}{\mathrm{d}x}+Y_{11}\frac{\mathrm{d}\varphi}{\mathrm{d}x}\right] \tag{36}$$

$$\int_A\left(D_z-\mu^2\frac{\mathrm{d}^2D_z}{\mathrm{d}x^2}\right)\beta\sin(\beta z)\,\mathrm{d}A=\left(1-l^2\nabla^2\right)\left[E_{31}\frac{\mathrm{d}\theta}{\mathrm{d}x}-c_1F_{31}\left(\frac{\mathrm{d}\theta}{\mathrm{d}x}+\frac{\mathrm{d}^2w}{\mathrm{d}x^2}\right)-X_{33}\phi-Y_{33}\varphi\right] \tag{37}$$

$$\int_A\left(B_x-\mu^2\frac{\mathrm{d}^2B_x}{\mathrm{d}x^2}\right)\cos(\beta z)\,\mathrm{d}A=\left(1-l^2\nabla^2\right)\left[(Q_{15}-c_2G_{15})\left(\theta+\frac{\mathrm{d}w}{\mathrm{d}x}\right)+Y_{11}\frac{\mathrm{d}\phi}{\mathrm{d}x}+T_{11}\frac{\mathrm{d}\varphi}{\mathrm{d}x}\right] \tag{38}$$

$$\int_A\left(B_z-\mu^2\frac{d^2B_z}{dx^2}\right)\beta\sin(\beta z)\mathrm{d}A=\left(1-l^2\nabla^2\right)\left[Q_{31}\frac{\mathrm{d}\theta}{\mathrm{d}x}-c_1G_{31}\left(\frac{\mathrm{d}\theta}{\mathrm{d}x}+\frac{\mathrm{d}^2w}{\mathrm{d}x^2}\right)-Y_{33}\phi-T_{33}\varphi\right] \tag{39}$$

Herein, the coefficients appearing in Eqs. (31)-(39) can be recalculated by

$$\begin{array}{l}
(A_{11},B_{11},D_{11},E_{11},F_{11},H_{11})=\int_A c_{11}\{1,z-z_0,\left(z-z_0\right)^2,z^3-c_0,\left(z-z_0\right)\left(z^3-c_0\right),\left(z^3-c_0\right)^2\}\mathrm{d}A;\\
(A_{55},D_{55},F_{55})=\int_A c_{55}\{1,z^2,z^4\}\mathrm{d}A;\left(N_T,M_T,P_T\right)=\int_A c_{11}\alpha_f(z)\Delta T\left(1,z-z_0,z^3-c_0\right)\mathrm{d}A;\\
\left(N_E,M_E,P_E\right)=-\int_A\frac{2e_{31}V_0}{h}\left(1,z-z_0,z^3-c_0\right)\mathrm{d}A;\left(N_H,M_H,P_H\right)=-\int_A\frac{2q_{31}\Omega}{h}\left(1,z-z_0,z^3-c_0\right)\mathrm{d}A;\\
(E_{31},F_{31})=\int_A e_{31}\beta\sin(\beta z)\left(z-z_0,z^3-c_0\right)\mathrm{d}A;\left(Q_{31},G_{31}\right)=\int_A q_{31}\beta\sin(\beta z)\left(z-z_0,z^3-c_0\right)\mathrm{d}A;\\
\left(X_{11},Y_{11},T_{11}\right)=\int_A\left(s_{11},d_{11},X_{11}\right)\cos^2(\beta z)\mathrm{d}A;\left(X_{33},Y_{33},T_{33}\right)=\int_A\left(s_{33},d_{33},X_{33}\right)\left[\beta\sin(\beta z)\right]^2\mathrm{d}A;\\
(E_{15},F_{15})=\int_A e_{15}\cos(\beta z)\{1,z^2\}\mathrm{d}A;\left(Q_{15},G_{15}\right)=\int_A q_{15}\cos(\beta z)\{1,z^2\}\mathrm{d}A;
\end{array}$$

The governing equations of the PFGMTEEMs nano-beams proposed in Eqs. (26)-(30) can be reformulated as

$$\begin{array}{l}\delta\theta:r_5\frac{\mathrm{d}w}{\mathrm{d}x}\frac{\mathrm{d}^2w}{\mathrm{d}x^2}+r_6\frac{\mathrm{d}^2\theta}{\mathrm{d}x^2}+r_7\frac{\mathrm{d}^3w}{\mathrm{d}x^3}+r_8\left(\theta+\frac{\mathrm{d}w}{\mathrm{d}x}\right)+r_9\frac{\mathrm{d}\phi}{\mathrm{d}x}+r_{10}\frac{\mathrm{d}\varphi}{\mathrm{d}x}\\ -l^2\left[r_5\left(3\frac{\mathrm{d}^3w}{\mathrm{d}x^3}\frac{\mathrm{d}^2w}{\mathrm{d}x^2}+\frac{\mathrm{d}w}{\mathrm{d}x}\frac{\mathrm{d}^4w}{\mathrm{d}x^4}\right)+r_6\frac{\mathrm{d}^4\theta}{\mathrm{d}x^4}+r_7\frac{\mathrm{d}^5w}{\mathrm{d}x^5}+r_8\left(\frac{\mathrm{d}^2\theta}{\mathrm{d}x^2}+\frac{\mathrm{d}^3w}{\mathrm{d}x^3}\right)+r_9\frac{\mathrm{d}^3\phi}{\mathrm{d}x^3}+r_{10}\frac{\mathrm{d}^3\varphi}{\mathrm{d}x^3}\right]=0\end{array} \tag{40}$$

$$\begin{array}{l}\delta\phi:r_1\frac{\mathrm{d}\theta}{\mathrm{d}x}+r_2\frac{\mathrm{d}^2w}{\mathrm{d}x^2}-X_{33}\phi-Y_{33}\varphi+X_{11}\frac{\mathrm{d}^2\phi}{\mathrm{d}x^2}+Y_{11}\frac{\mathrm{d}^2\varphi}{\mathrm{d}x^2}\\ -l^2\left(r_1\frac{\mathrm{d}^3\theta}{\mathrm{d}x^3}+r_2\frac{\mathrm{d}^4w}{\mathrm{d}x^4}-X_{33}\frac{\mathrm{d}^2\phi}{\mathrm{d}x^2}-Y_{33}\frac{\mathrm{d}^2\varphi}{\mathrm{d}x^2}+X_{11}\frac{\mathrm{d}^4\phi}{\mathrm{d}x^4}+Y_{11}\frac{\mathrm{d}^4\varphi}{\mathrm{d}x^4}\right)=0\end{array} \tag{41}$$

$$\begin{array}{l}\delta\varphi:r_3\frac{\mathrm{d}\theta}{\mathrm{d}x}+r_4\frac{\mathrm{d}^2w}{\mathrm{d}x^2}-Y_{33}\phi-T_{33}\varphi+Y_{11}\frac{\mathrm{d}^2\phi}{\mathrm{d}x^2}+T_{11}\frac{\mathrm{d}^2\varphi}{\mathrm{d}x^2}\\ -l^2\left(r_3\frac{\mathrm{d}^3\theta}{\mathrm{d}x^3}+r_4\frac{\mathrm{d}^4w}{\mathrm{d}x^4}-Y_{33}\frac{\mathrm{d}^2\phi}{\mathrm{d}x^2}-T_{33}\frac{\mathrm{d}^2\varphi}{\mathrm{d}x^2}+Y_{11}\frac{\mathrm{d}^4\phi}{\mathrm{d}x^4}+T_{11}\frac{\mathrm{d}^4\varphi}{\mathrm{d}x^4}\right)=0\end{array} \tag{42}$$

$$\begin{array}{l}\delta w:\left[N-(N_E+N_H+N_T)\right]\left(\frac{\mathrm{d}^2w}{\mathrm{d}x^2}-\mu^2\frac{\mathrm{d}^4w}{\mathrm{d}x^4}\right)+q-r_8\left(\frac{\mathrm{d}\theta}{\mathrm{d}x}+\frac{\mathrm{d}^2w}{\mathrm{d}x^2}\right)-r_2\frac{\mathrm{d}^2\phi}{\mathrm{d}x^2}-r_4\frac{\mathrm{d}^2\varphi}{\mathrm{d}x^2}-c_1^2H_{11}\frac{\mathrm{d}^4w}{\mathrm{d}x^4}\\ -l^2\left[\begin{array}{l}c_1E_{11}\left(3\frac{\mathrm{d}^2w}{\mathrm{d}x^2}\frac{\mathrm{d}^3w}{\mathrm{d}x^3}+4\frac{\mathrm{d}^2w}{\mathrm{d}x^2}\frac{\mathrm{d}^4w}{\mathrm{d}x^4}+\frac{\mathrm{d}w}{\mathrm{d}x}\frac{\mathrm{d}^5w}{\mathrm{d}x^5}\right)-c_1^2H_{11}\frac{\mathrm{d}^6w}{\mathrm{d}x^6}\\ -r_8\left(\frac{\mathrm{d}^3\theta}{\mathrm{d}x^3}+\frac{\mathrm{d}^4w}{\mathrm{d}x^4}\right)-r_2\frac{\mathrm{d}^4\phi}{\mathrm{d}x^4}-r_4\frac{\mathrm{d}^4\varphi}{\mathrm{d}x^4}-r_7\frac{\mathrm{d}^5\theta}{\mathrm{d}x^5}\end{array}\right]-r_7\frac{\mathrm{d}^3\theta}{\mathrm{d}x^3}+c_1E_{11}\left[\left(\frac{\mathrm{d}^2w}{\mathrm{d}x^2}\right)^2+\frac{\mathrm{d}w}{\mathrm{d}x}\frac{\mathrm{d}^3w}{\mathrm{d}x^3}\right]=0\end{array} \tag{43}$$

in which

$$\begin{array}{l}
r_1=E_{31}-c_1F_{31}+E_{15}-c_2F_{15};r_2=E_{15}-c_2F_{15}-c_1F_{31};r_3=Q_{31}-c_1G_{31}+Q_{15}-c_2G_{15};r_5=B_{11}-c_1E_{11};\\
r_4=Q_{15}-c_2G_{15}-c_1G_{31};r_6=D_{11}-2c_1F_{11}+c_1^2H_{11};r_7=c_1^2H_{11}-c_1F_{11};r_{10}=Q_{31}+Q_{15}-c_1G_{31}-c_2G_{15};\\
r_8=2c_2D_{55}-c_2^2F_{55}-A_{55};r_9=E_{31}+E_{15}-c_2F_{15}-c_1F_{31};
\end{array}$$

It is indicated from Eq. (26) that N is a constant.

$$N=\frac{1}{L}\int_0^L\left\{\begin{array}{l}\frac{A_{11}}{2}\left(\frac{\mathrm{d}w}{\mathrm{d}x}\right)^2+B_{11}\frac{\mathrm{d}\theta}{\mathrm{d}x}-c_1E_{11}\left(\frac{\mathrm{d}\theta}{\mathrm{d}x}+\frac{\mathrm{d}^2w}{\mathrm{d}x^2}\right)\\ -l^2\left[A_{11}\left(\frac{\mathrm{d}w}{\mathrm{d}x}\frac{\mathrm{d}^3w}{\mathrm{d}x^3}+\frac{\mathrm{d}^2w}{\mathrm{d}x^2}\frac{\mathrm{d}^2w}{\mathrm{d}x^2}\right)+B_{11}\frac{\mathrm{d}^3\theta}{\mathrm{d}x^3}-c_1E_{11}\left(\frac{\mathrm{d}^3\theta}{\mathrm{d}x^3}+\frac{\mathrm{d}^4w}{\mathrm{d}x^4}\right)\right]\end{array}\right\}\mathrm{d}x-N_E-N_H-N_T$$

In the actual project, multiple physical fields, including the temperature field, the electric field, the magnetic field and the stress field, are interacted on each other at the boundary conditions of the PFGMTEEMs beams, which is a typical multiple fields coupling problem. To date, no research has explored the original boundary conditions of beams made of functionally graded magneto-thermo-electro-elastic materials. Thus, we introduce the concept of the simplified boundary condition (Dehrouyeh-Semnani 2017) to establish the equivalent boundary conditions of PFGMTEEMs nanobeams.

For simply supported ends (*S-S*):

$$X=0,L;u=0,w=0,M=0,P=0,\phi=0,\varphi=0; \tag{44}$$

For immovable clamped ends (*C-C*):

$$X=0,L;u=0,w=0,\theta=0,\phi=0,\varphi=0; \tag{45}$$

Next, we begin to introduce the following dimensionless parameters in order to make the calculation as quickly and compactly as possible.

$$\begin{aligned}
&\xi=\frac{x}{L}\pi,\bar{w}=\frac{w}{L},\bar{\theta}=\frac{\theta}{\pi},\bar{\phi}=\frac{\phi}{\phi_0},\phi_0=\sqrt{\frac{A_{11}}{X_{33}}},\varphi_0=\sqrt{\frac{A_{11}}{T_{33}}},\bar{\varphi}=\frac{\varphi}{\varphi_0},\left(\bar{T}_{11},\bar{T}_{33}\right)=\left(\frac{T_{11}\varphi_0^2\pi^2}{SL^2},\frac{T_{33}\varphi_0^2}{S}\right),\bar{l}=\frac{l}{L}\pi,\\
&(\bar{A}_{11},\bar{B}_{11},\bar{E}_{11},\bar{D}_{11},\bar{F}_{11},\bar{H}_{11})=\left(\frac{A_{11}}{S},\frac{B_{11}\pi}{SL},\frac{E_{11}\pi^3}{SL^3},\frac{D_{11}\pi^2}{SL^2},\frac{F_{11}\pi^4}{SL^4},\frac{H_{11}\pi^6}{SL^6}\right),(\bar{X}_{11},\bar{X}_{33})=\left(\frac{X_{11}\phi_0^2\pi^2}{SL^2},\frac{X_{33}\phi_0^2}{A_{11}}\right),\\
&(\bar{N}_T,\bar{N}_E,\bar{N}_H)=\left(\frac{N_T}{S},\frac{N_E}{S},\frac{N_H}{S}\right),(\bar{A}_{55},\bar{D}_{55},\bar{F}_{55})=\left(\frac{A_{55}}{S},\frac{D_{55}\pi^2}{SL^2},\frac{F_{55}\pi^4}{SL^4}\right),(\bar{c}_1,\bar{c}_2)=(c_1,c_2)\frac{L^2}{\pi^2},\lambda_q=\frac{qL^2}{S\pi^2},\\
&(\bar{E}_{15},\bar{E}_{31},\bar{F}_{15},\bar{F}_{31})=\left(\frac{E_{15}\phi_0\pi}{SL},\frac{E_{31}\phi_0\pi}{SL},\frac{F_{15}\phi_0\pi^3}{SL^3},\frac{F_{31}\phi_0\pi^3}{SL^3}\right),\left(\bar{Y}_{11},\bar{Y}_{33}\right)=\left(\frac{Y_{11}\phi_0\varphi_0\pi^2}{SL^2},\frac{Y_{33}\phi_0\varphi_0}{S}\right),\bar{\mu}=\frac{\mu}{L}\pi,\\
&\left(\bar{Q}_{15},\bar{Q}_{31},\bar{G}_{15},\bar{G}_{31}\right)=\left(\frac{Q_{15}\varphi_0\pi}{SL},\frac{Q_{31}\varphi_0\pi}{SL},\frac{G_{15}\varphi_0\pi^3}{SL^3},\frac{G_{31}\varphi_0\pi^3}{SL^3}\right),S=\int_A c_{11}\mathrm{d}z\mathrm{d}y,
\end{aligned}$$

General governing equations proposed in Eqs. (40)-(43) can be rewritten as

$$\begin{aligned}
&\delta\bar{\theta}:\bar{r}_5\frac{\mathrm{d}\bar{w}}{\mathrm{d}\xi}\frac{\mathrm{d}^2\bar{w}}{\mathrm{d}\xi^2}+\bar{r}_6\frac{\mathrm{d}^2\bar{\theta}}{\mathrm{d}\xi^2}+\bar{r}_7\frac{\mathrm{d}^3\bar{w}}{\mathrm{d}\xi^3}+\bar{r}_8\left(\bar{\theta}+\frac{\mathrm{d}\bar{w}}{\mathrm{d}\xi}\right)+\bar{r}_9\frac{\mathrm{d}\bar{\phi}}{\mathrm{d}\xi}+\bar{r}_{10}\frac{\mathrm{d}\bar{\varphi}}{\mathrm{d}\xi}\\
&-\bar{l}^2\left[\bar{r}_5\left(3\frac{\mathrm{d}^3\bar{w}}{\mathrm{d}\xi^3}\frac{\mathrm{d}^2\bar{w}}{\mathrm{d}\xi^2}+\frac{\mathrm{d}\bar{w}}{\mathrm{d}\xi}\frac{\mathrm{d}^4\bar{w}}{\mathrm{d}\xi^4}\right)+\bar{r}_6\frac{\mathrm{d}^4\bar{\theta}}{\mathrm{d}\xi^4}+\bar{r}_7\frac{\mathrm{d}^5\bar{w}}{\mathrm{d}\xi^5}+\bar{r}_8\left(\frac{\mathrm{d}^2\bar{\theta}}{\mathrm{d}\xi^2}+\frac{\mathrm{d}^3\bar{w}}{\mathrm{d}\xi^3}\right)+\bar{r}_9\frac{\mathrm{d}^3\bar{\phi}}{\mathrm{d}\xi^3}+\bar{r}_{10}\frac{\mathrm{d}^3\bar{\varphi}}{\mathrm{d}\xi^3}\right]=0
\end{aligned} \tag{46}$$

$$\begin{aligned}
&\delta\bar{\phi}:\bar{r}_1\frac{\mathrm{d}\bar{\theta}}{\mathrm{d}\xi}+\bar{r}_2\frac{\mathrm{d}^2\bar{w}}{\mathrm{d}\xi^2}-\bar{X}_{33}\bar{\phi}-\bar{Y}_{33}\bar{\varphi}+\bar{X}_{11}\frac{\mathrm{d}^2\bar{\phi}}{\mathrm{d}\xi^2}+\bar{Y}_{11}\frac{\mathrm{d}^2\bar{\varphi}}{\mathrm{d}\xi^2}\\
&-\bar{l}^2\left(\bar{r}_1\frac{\mathrm{d}^3\bar{\theta}}{\mathrm{d}\xi^3}+\bar{r}_2\frac{\mathrm{d}^4\bar{w}}{\mathrm{d}\xi^4}-\bar{X}_{33}\frac{\mathrm{d}^2\bar{\phi}}{\mathrm{d}\xi^2}-\bar{Y}_{33}\frac{\mathrm{d}^2\bar{\varphi}}{\mathrm{d}\xi^2}+\bar{X}_{11}\frac{\mathrm{d}^4\bar{\phi}}{\mathrm{d}\xi^4}+\bar{Y}_{11}\frac{\mathrm{d}^4\bar{\varphi}}{\mathrm{d}\xi^4}\right)=0
\end{aligned} \tag{47}$$

$$\begin{aligned}
&\delta\bar{\varphi}:\bar{r}_3\frac{\mathrm{d}\bar{\theta}}{\mathrm{d}\xi}+\bar{r}_4\frac{\mathrm{d}^2\bar{w}}{\mathrm{d}\xi^2}-\bar{Y}_{33}\bar{\phi}-\bar{T}_{33}\bar{\varphi}+\bar{Y}_{11}\frac{\mathrm{d}^2\bar{\phi}}{\mathrm{d}\xi^2}+\bar{T}_{11}\frac{\mathrm{d}^2\bar{\varphi}}{\mathrm{d}\xi^2}\\
&-\bar{l}^2\left(\bar{r}_3\frac{\mathrm{d}^3\bar{\theta}}{\mathrm{d}\xi^3}+\bar{r}_4\frac{\mathrm{d}^4\bar{w}}{\mathrm{d}\xi^4}-\bar{Y}_{33}\frac{\mathrm{d}^2\bar{\phi}}{\mathrm{d}\xi^2}-\bar{T}_{33}\frac{\mathrm{d}^2\bar{\varphi}}{\mathrm{d}\xi^2}+\bar{Y}_{11}\frac{\mathrm{d}^4\bar{\phi}}{\mathrm{d}\xi^4}+\bar{T}_{11}\frac{\mathrm{d}^4\bar{\varphi}}{\mathrm{d}\xi^4}\right)=0
\end{aligned} \tag{48}$$

$$\begin{aligned}
&\delta\bar{w}:\left[\bar{N}-(\bar{N}_E+\bar{N}_H+\bar{N}_T)\right]\left(\frac{\mathrm{d}^2\bar{w}}{\mathrm{d}\xi^2}-\bar{\mu}^2\frac{\mathrm{d}^4\bar{w}}{\mathrm{d}\xi^4}\right)+\lambda_q-\frac{\bar{r}_8}{\pi}\left(\frac{\mathrm{d}\bar{\theta}}{\mathrm{d}\xi}+\frac{\mathrm{d}^2\bar{w}}{\mathrm{d}\xi^2}\right)-\frac{\bar{r}_2}{\pi^2}\frac{\mathrm{d}^2\bar{\phi}}{\mathrm{d}\xi^2}-\frac{\bar{r}_4}{\pi^2}\frac{\mathrm{d}^2\bar{\varphi}}{\mathrm{d}\xi^2}-\bar{c}_1^2\bar{H}_{11}\frac{\mathrm{d}^4\bar{w}}{\mathrm{d}\xi^4}\\
&-\bar{l}^2\begin{bmatrix}\bar{c}_1\bar{E}_{11}\pi\left(3\frac{\mathrm{d}^2\bar{w}}{\mathrm{d}\xi^2}\frac{\mathrm{d}^3\bar{w}}{\mathrm{d}\xi^3}+4\frac{\mathrm{d}^2\bar{w}}{\mathrm{d}\xi^2}\frac{\mathrm{d}^4\bar{w}}{\mathrm{d}\xi^4}+\frac{\mathrm{d}\bar{w}}{\mathrm{d}\xi}\frac{\mathrm{d}^5\bar{w}}{\mathrm{d}\xi^5}\right)-\bar{c}_1^2\bar{H}_{11}\frac{\mathrm{d}^6\bar{w}}{\mathrm{d}\xi^6}\\-\frac{\bar{r}_8}{\pi}\left(\frac{\mathrm{d}^3\bar{\theta}}{\mathrm{d}\xi^3}+\frac{\mathrm{d}^4\bar{w}}{\mathrm{d}\xi^4}\right)-\frac{\bar{r}_2}{\pi^2}\frac{\mathrm{d}^4\bar{\phi}}{\mathrm{d}\xi^4}-\frac{\bar{r}_4}{\pi^2}\frac{\mathrm{d}^4\bar{\varphi}}{\mathrm{d}\xi^4}-\frac{\bar{r}_7}{\pi}\frac{\mathrm{d}^5\bar{\theta}}{\mathrm{d}\xi^5}\end{bmatrix}+\pi\bar{c}_1\bar{E}_{11}\left[\left(\frac{\mathrm{d}^2\bar{w}}{\mathrm{d}\xi^2}\right)^2+\frac{\mathrm{d}\bar{w}}{\mathrm{d}\xi}\frac{\mathrm{d}^3\bar{w}}{\mathrm{d}\xi^3}\right]\\
&-\frac{\bar{r}_7}{\pi}\frac{\mathrm{d}^3\bar{\theta}}{\mathrm{d}\xi^3}=0
\end{aligned} \tag{49}$$

where

$$\begin{aligned}
&\bar{r}_1=\pi\left(\bar{E}_{31}-\bar{c}_1\bar{F}_{31}+\bar{E}_{15}-\bar{c}_2\bar{F}_{15}\right);\bar{r}_2=\pi\left(\bar{E}_{15}-\bar{c}_2\bar{F}_{15}-\bar{c}_1\bar{F}_{31}\right);\bar{r}_3=\pi\left(\bar{Q}_{31}-\bar{c}_1\bar{G}_{31}+\bar{Q}_{15}-\bar{c}_2\bar{G}_{15}\right);\\
&\bar{r}_4=\pi\left(\bar{Q}_{15}-\bar{c}_2\bar{G}_{15}-\bar{c}_1\bar{G}_{31}\right);\bar{r}_6=\pi\left(\bar{D}_{11}-2\bar{c}_1\bar{F}_{11}+\bar{c}_1^2\bar{H}_{11}\right);\bar{r}_7=\pi\left(\bar{c}_1^2\bar{H}_{11}-\bar{c}_1\bar{F}_{11}\right);\bar{r}_5=\pi^2\left(\bar{B}_{11}-\bar{c}_1\bar{E}_{11}\right);\\
&\bar{r}_8=\pi\left(2\bar{c}_2\bar{D}_{55}-\bar{c}_2^2\bar{F}_{55}-\bar{A}_{55}\right);\bar{r}_9=\bar{E}_{31}+\bar{E}_{15}-\bar{c}_2\bar{F}_{15}-\bar{c}_1\bar{F}_{31};\bar{r}_{10}=\bar{Q}_{31}+\bar{Q}_{15}-\bar{c}_1\bar{G}_{31}-\bar{c}_2\bar{G}_{15};\\
&\bar{N}=\int_0^\pi\left\{\begin{aligned}&\frac{\bar{A}_{11}\pi}{2}\left(\frac{\mathrm{d}\bar{w}}{\mathrm{d}\xi}\right)^{2}+\bar{B}_{11}\frac{\mathrm{d}\bar{\theta}}{\mathrm{d}\xi}-\bar{c}_1\bar{E}_{11}\left(\frac{\mathrm{d}\bar{\theta}}{\mathrm{d}\xi}+\frac{\mathrm{d}^2\bar{w}}{\mathrm{d}\xi^2}\right)\\&-\bar{l}^2\left[\bar{A}_{11}\pi\left(\frac{\mathrm{d}\bar{w}}{\mathrm{d}\xi}\frac{\mathrm{d}^3\bar{w}}{\mathrm{d}\xi^3}+\frac{\mathrm{d}^2\bar{w}}{\mathrm{d}\xi^2}\frac{\mathrm{d}^2\bar{w}}{\mathrm{d}\xi^2}\right)+\bar{B}_{11}\frac{\mathrm{d}^3\bar{\theta}}{\mathrm{d}\xi^3}-\bar{c}_1\bar{E}_{11}\left(\frac{\mathrm{d}^3\bar{\theta}}{\mathrm{d}\xi^3}+\frac{\mathrm{d}^4\bar{w}}{\mathrm{d}\xi^4}\right)\right]\end{aligned}\right\}\mathrm{d}\xi-\bar{N}_E-\bar{N}_H-\bar{N}_T
\end{aligned}$$

The dimensionless boundary conditions of the PFGMTEEMs nanobeams can be extracted as

- For simply supported ends (*S-S*):

$$\xi=0,\pi;\bar{u}=0,\bar{w}=0,\bar{M}=0,\bar{P}=0,\bar{\phi}=0,\bar{\varphi}=0; \tag{50}$$

- For immovable clamped ends (*C-C*):

$$\xi=0,\pi;\bar{u}=0,\bar{w}=0,\bar{\theta}=0,\bar{\phi}=0,\bar{\varphi}=0; \tag{51}$$

4. Method of solution

In this section, to obtain corresponding analytical solutions, an improved perturbation method called a two-step perturbation technique is introduced to resolve the nonlinear governing equations. Before seriously acquiring a set of perturbation equations, the expanded forms of dimensionless displacement, dimensionless rotation angle, dimensionless transverse load, dimensionless electric potential, dimensionless magnetic potential are assumed to be

$$\begin{aligned}
&\bar{w}(\xi,\varepsilon)=\sum_{n=1}\varepsilon^n w_n(\xi);\bar{\theta}(\xi,\varepsilon)=\sum_{n=1}\varepsilon^n\bar{\theta}_n(\xi);\lambda_q(\xi,\varepsilon)=\sum_{n=1}\varepsilon^n\lambda_q^n(\xi);\bar{\phi}(\xi,\varepsilon)=\sum_{n=1}\varepsilon^n\bar{\phi}_n(\xi);\\
&\bar{\varphi}\left(\xi,\varepsilon\right)=\sum_{n=0}\varepsilon^n\varphi_n(\xi);
\end{aligned} \tag{52}$$

It should be noted that the small perturbation parameter ε in Eq. (52) has no additional physical significance. Via substituting Eq. (52) into Eqs. (46)-(49), then collecting terms of the same order ε, we get

$O(\varepsilon^1)$:

$$\begin{aligned}
&\bar{r}_1\frac{\mathrm{d}\bar{\theta}_1}{\mathrm{d}\xi}+\bar{r}_2\frac{\mathrm{d}^2\bar{w}_1}{\mathrm{d}\xi^2}-\bar{X}_{33}\bar{\phi}_1-\bar{Y}_{33}\bar{\varphi}_1+\bar{X}_{11}\frac{\mathrm{d}^2\bar{\phi}_1}{\mathrm{d}\xi^2}+\bar{Y}_{11}\frac{\mathrm{d}^2\bar{\varphi}_1}{\mathrm{d}\xi^2}\\
&-\bar{l}^2\left(\bar{r}_1\frac{\mathrm{d}^3\bar{\theta}_1}{\mathrm{d}\xi^3}+\bar{r}_2\frac{\mathrm{d}^4\bar{w}_1}{\mathrm{d}\xi^4}-\bar{X}_{33}\frac{\mathrm{d}^2\bar{\phi}_1}{\mathrm{d}\xi^2}-\bar{Y}_{33}\frac{\mathrm{d}^2\bar{\varphi}_1}{\mathrm{d}\xi^2}+\bar{X}_{11}\frac{\mathrm{d}^4\bar{\phi}_1}{\mathrm{d}\xi^4}+\bar{Y}_{11}\frac{\mathrm{d}^4\bar{\varphi}_1}{\mathrm{d}\xi^4}\right)=0
\end{aligned} \tag{53}$$

$$\begin{aligned}
&\bar{r}_3\frac{\mathrm{d}\bar{\theta}_1}{\mathrm{d}\xi}+\bar{r}_4\frac{\mathrm{d}^2\bar{w}_1}{\mathrm{d}\xi^2}-\bar{Y}_{33}\bar{\phi}_1-\bar{T}_{33}\bar{\varphi}_1+\bar{Y}_{11}\frac{\mathrm{d}^2\bar{\phi}_1}{\mathrm{d}\xi^2}+\bar{T}_{11}\frac{\mathrm{d}^2\bar{\varphi}_1}{\mathrm{d}\xi^2}\\
&-\bar{l}^2\left(\bar{r}_3\frac{\mathrm{d}^3\bar{\theta}_1}{\mathrm{d}\xi^3}+\bar{r}_4\frac{\mathrm{d}^4\bar{w}_1}{\mathrm{d}\xi^4}-\bar{Y}_{33}\frac{\mathrm{d}^2\bar{\phi}_1}{\mathrm{d}\xi^2}-\bar{T}_{33}\frac{\mathrm{d}^2\bar{\varphi}_1}{\mathrm{d}\xi^2}+\bar{Y}_{11}\frac{\mathrm{d}^4\bar{\phi}_1}{\mathrm{d}\xi^4}+\bar{T}_{11}\frac{\mathrm{d}^4\bar{\varphi}_1}{\mathrm{d}\xi^4}\right)=0
\end{aligned} \tag{54}$$

$$\begin{aligned}
&\bar{r}_6\frac{\mathrm{d}^2\bar{\theta}_1}{\mathrm{d}\xi^2}+\bar{r}_7\frac{\mathrm{d}^3\bar{w}_1}{\mathrm{d}\xi^3}+\bar{r}_8\left(\bar{\theta}_1+\frac{\mathrm{d}\bar{w}_1}{\mathrm{d}\xi}\right)+\bar{r}_9\frac{\mathrm{d}\bar{\phi}_1}{\mathrm{d}\xi}+\bar{r}_{10}\frac{\mathrm{d}\bar{\varphi}_1}{\mathrm{d}\xi}\\
&-\bar{l}^2\left[\bar{r}_6\frac{\mathrm{d}^4\bar{\theta}_1}{\mathrm{d}\xi^4}+\bar{r}_7\frac{\mathrm{d}^5\bar{w}_1}{\mathrm{d}\xi^5}+\bar{r}_8\left(\frac{\mathrm{d}^2\bar{\theta}_1}{\mathrm{d}\xi^2}+\frac{\mathrm{d}^3\bar{w}_1}{\mathrm{d}\xi^3}\right)+\bar{r}_9\frac{\mathrm{d}^3\bar{\phi}_1}{\mathrm{d}\xi^3}+\bar{r}_{10}\frac{\mathrm{d}^3\bar{\varphi}_1}{\mathrm{d}\xi^3}\right]=0
\end{aligned} \tag{55}$$

$$\begin{aligned}
&\lambda_q^1-2(\bar{N}_E+\bar{N}_H+\bar{N}_T)\left(\frac{\mathrm{d}^2\bar{w}_1}{\mathrm{d}\xi^2}-\bar{\mu}^2\frac{\mathrm{d}^4\bar{w}_1}{\mathrm{d}\xi^4}\right)-\frac{\bar{r}_8}{\pi}\left(\frac{\mathrm{d}\bar{\theta}_1}{\mathrm{d}\xi}+\frac{\mathrm{d}^2\bar{w}_1}{\mathrm{d}\xi^2}\right)-\frac{\bar{r}_2}{\pi^2}\frac{\mathrm{d}^2\bar{\phi}_1}{\mathrm{d}\xi^2}-\frac{\bar{r}_4}{\pi^2}\frac{\mathrm{d}^2\bar{\varphi}_1}{\mathrm{d}\xi^2}-\bar{c}_1^2\bar{H}_{11}\frac{\mathrm{d}^4\bar{w}_1}{\mathrm{d}\xi^4}\\
&-\bar{l}^2\left[-\bar{c}_1^2\bar{H}_{11}\frac{\mathrm{d}^6\bar{w}_1}{\mathrm{d}\xi^6}-\frac{\bar{r}_8}{\pi}\left(\frac{\mathrm{d}^3\bar{\theta}_1}{\mathrm{d}\xi^3}+\frac{\mathrm{d}^4\bar{w}_1}{\mathrm{d}\xi^4}\right)-\frac{\bar{r}_2}{\pi^2}\frac{\mathrm{d}^4\bar{\phi}_1}{\mathrm{d}\xi^4}-\frac{\bar{r}_4}{\pi^2}\frac{\mathrm{d}^4\bar{\varphi}_1}{\mathrm{d}\xi^4}-\frac{\bar{r}_7}{\pi}\frac{\mathrm{d}^5\bar{\theta}_1}{\mathrm{d}\xi^5}\right]-\frac{\bar{r}_7}{\pi}\frac{\mathrm{d}^3\bar{\theta}_1}{\mathrm{d}\xi^3}=0
\end{aligned} \tag{56}$$

$O(\varepsilon^2)$:

$$\begin{aligned}
&\bar{r}_1\frac{\mathrm{d}\bar{\theta}_2}{\mathrm{d}\xi}+\bar{r}_2\frac{\mathrm{d}^2\bar{w}_2}{\mathrm{d}\xi^2}-\bar{X}_{33}\bar{\phi}_2-\bar{Y}_{33}\bar{\varphi}_2+\bar{X}_{11}\frac{\mathrm{d}^2\bar{\phi}_2}{\mathrm{d}\xi^2}+\bar{Y}_{11}\frac{\mathrm{d}^2\bar{\varphi}_2}{\mathrm{d}\xi^2}\\
&-\bar{l}^2\left(\bar{r}_1\frac{\mathrm{d}^3\bar{\theta}_2}{\mathrm{d}\xi^3}+\bar{r}_2\frac{\mathrm{d}^4\bar{w}_2}{\mathrm{d}\xi^4}-\bar{X}_{33}\frac{\mathrm{d}^2\bar{\phi}_2}{\mathrm{d}\xi^2}-\bar{Y}_{33}\frac{\mathrm{d}^2\bar{\varphi}_2}{\mathrm{d}\xi^2}+\bar{X}_{11}\frac{\mathrm{d}^4\bar{\phi}_2}{\mathrm{d}\xi^4}+\bar{Y}_{11}\frac{\mathrm{d}^4\bar{\varphi}_2}{\mathrm{d}\xi^4}\right)=0
\end{aligned} \tag{57}$$

$$\begin{aligned}&\bar{r}_3\frac{d\bar{\theta}_2}{d\xi}+\bar{r}_4\frac{d^2\bar{w}_2}{d\xi^2}-\bar{Y}_{33}\bar{\phi}_2-\bar{T}_{33}\bar{\varphi}_2+\bar{Y}_{11}\frac{d^2\bar{\phi}_2}{d\xi^2}+\bar{T}_{11}\frac{d^2\bar{\varphi}_2}{d\xi^2}\\&-\bar{l}^2\left(\bar{r}_3\frac{d^3\bar{\theta}_2}{d\xi^3}+\bar{r}_4\frac{d^4\bar{w}_2}{d\xi^4}-\bar{Y}_{33}\frac{d^2\bar{\phi}_2}{d\xi^2}-\bar{T}_{33}\frac{d^2\bar{\varphi}_2}{d\xi^2}+\bar{Y}_{11}\frac{d^4\bar{\phi}_2}{d\xi^4}+\bar{T}_{11}\frac{d^4\bar{\varphi}_2}{d\xi^4}\right)=0\end{aligned}\tag{58}$$

$$\begin{aligned}&\bar{r}_5\frac{d\bar{w}_1}{d\xi}\frac{d^2\bar{w}_1}{d\xi^2}+\bar{r}_6\frac{d^2\bar{\theta}_2}{d\xi^2}+\bar{r}_7\frac{d^3\bar{w}_2}{d\xi^3}+\bar{r}_8\left(\bar{\theta}_2+\frac{d\bar{w}_2}{d\xi}\right)+\bar{r}_9\frac{d\bar{\phi}_2}{d\xi}+\bar{r}_{10}\frac{d\bar{\varphi}_2}{d\xi}\\&-\bar{l}^2\left[\bar{r}_5\left(3\frac{d^3\bar{w}_1}{d\xi^3}\frac{d^2\bar{w}_1}{d\xi^2}+\frac{d\bar{w}_1}{d\xi}\frac{d^4\bar{w}_1}{d\xi^4}\right)+\bar{r}_6\frac{d^4\bar{\theta}_2}{d\xi^4}+\bar{r}_7\frac{d^5\bar{w}_2}{d\xi^5}+\bar{r}_8\left(\frac{d^2\bar{\theta}_2}{d\xi^2}+\frac{d^3\bar{w}_2}{d\xi^3}\right)+\bar{r}_9\frac{d^3\bar{\phi}_2}{d\xi^3}+\bar{r}_{10}\frac{d^3\bar{\varphi}_2}{d\xi^3}\right]=0\end{aligned}\tag{59}$$

$$\begin{aligned}&\int_0^{\pi}\bar{B}_{11}\frac{d\bar{\theta}_1}{d\xi}-\bar{c}_1\bar{E}_{11}\left(\frac{d\bar{\theta}_1}{d\xi}+\frac{d^2\bar{w}_1}{d\xi^2}\right)-\bar{l}^2\left[\bar{B}_{11}\frac{d^3\bar{\theta}_1}{d\xi^3}-\bar{c}_1\bar{E}_{11}\left(\frac{d^3\bar{\theta}_1}{d\xi^3}+\frac{d^4\bar{w}_1}{d\xi^4}\right)\right]d\xi\left(\frac{d^2\bar{w}_1}{d\xi^2}-\bar{\mu}^2\frac{d^4\bar{w}_1}{d\xi^4}\right)+\lambda_q^2\\&-2(\bar{N}_E+\bar{N}_H+\bar{N}_T)\left(\frac{d^2\bar{w}_2}{d\xi^2}-\bar{\mu}^2\frac{d^4\bar{w}_2}{d\xi^4}\right)-\frac{\bar{r}_8}{\pi}\left(\frac{d\bar{\theta}_2}{d\xi}+\frac{d^2\bar{w}_2}{d\xi^2}\right)-\frac{\bar{r}_2}{\pi^2}\frac{d^2\bar{\phi}_2}{d\xi^2}-\frac{\bar{r}_4}{\pi^2}\frac{d^2\bar{\varphi}_2}{d\xi^2}-\bar{c}_1^2\bar{H}_{11}\frac{d^4\bar{w}_2}{d\xi^4}\\&-\bar{l}^2\left[\begin{aligned}&\bar{c}_1\bar{E}_{11}\pi\left(3\frac{d^3\bar{w}_1}{d\xi^2}\frac{d^3\bar{w}_1}{d\xi^3}+4\frac{d^2\bar{w}_1}{d\xi^2}\frac{d^4\bar{w}_1}{d\xi^4}+\frac{d\bar{w}_1}{d\xi}\frac{d^5\bar{w}_1}{d\xi^5}\right)-\bar{c}_1^2\bar{H}_{11}\frac{d^6\bar{w}_2}{d\xi^6}\\&-\frac{\bar{r}_8}{\pi}\left(\frac{d^3\bar{\theta}_2}{d\xi^3}+\frac{d^4\bar{w}_2}{d\xi^4}\right)-\frac{\bar{r}_2}{\pi^2}\frac{d^4\bar{\phi}_2}{d\xi^4}-\frac{\bar{r}_4}{\pi^2}\frac{d^4\bar{\varphi}_2}{d\xi^4}-\frac{\bar{r}_7}{\pi}\frac{d^5\bar{\theta}_2}{d\xi^5}\end{aligned}\right]+\pi\bar{c}_1\bar{E}_{11}\left[\left(\frac{d^2\bar{w}_1}{d\xi^2}\right)^2+\frac{d\bar{w}_1}{d\xi}\frac{d^3\bar{w}_1}{d\xi^3}\right]\\&-\frac{\bar{r}_7}{\pi}\frac{d^3\bar{\theta}_2}{d\xi^3}=0\end{aligned}\tag{60}$$

$O(\varepsilon^3)$:

$$\begin{aligned}&\bar{r}_1\frac{d\bar{\theta}_3}{d\xi}+\bar{r}_2\frac{d^2\bar{w}_3}{d\xi^2}-\bar{X}_{33}\bar{\phi}_3-\bar{Y}_{33}\bar{\varphi}_3+\bar{X}_{11}\frac{d^2\bar{\phi}_3}{d\xi^2}+\bar{Y}_{11}\frac{d^2\bar{\varphi}_3}{d\xi^2}\\&-\bar{l}^2\left(\bar{r}_1\frac{d^3\bar{\theta}_3}{d\xi^3}+\bar{r}_2\frac{d^4\bar{w}_3}{d\xi^4}-\bar{X}_{33}\frac{d^2\bar{\phi}_3}{d\xi^2}-\bar{Y}_{33}\frac{d^2\bar{\varphi}_3}{d\xi^2}+\bar{X}_{11}\frac{d^4\bar{\phi}_3}{d\xi^4}+\bar{Y}_{11}\frac{d^4\bar{\varphi}_3}{d\xi^4}\right)=0\end{aligned}\tag{61}$$

$$\begin{aligned}&\bar{r}_3\frac{d\bar{\theta}_3}{d\xi}+\bar{r}_4\frac{d^2\bar{w}}{d\xi^2}-\bar{Y}_{33}\bar{\phi}_3-\bar{T}_{33}\bar{\varphi}_3+\bar{Y}_{11}\frac{d^2\bar{\phi}_3}{d\xi^2}+\bar{T}_{11}\frac{d^2\bar{\varphi}_3}{d\xi^2}\\&-\bar{l}^2\left(\bar{r}_3\frac{d^3\bar{\theta}_3}{d\xi^3}+\bar{r}_4\frac{d^4\bar{w}_3}{d\xi^4}-\bar{Y}_{33}\frac{d^2\bar{\phi}_3}{d\xi^2}-\bar{T}_{33}\frac{d^2\bar{\varphi}_3}{d\xi^2}+\bar{Y}_{11}\frac{d^4\bar{\phi}_3}{d\xi^4}+\bar{T}_{11}\frac{d^4\bar{\varphi}_3}{d\xi^4}\right)=0\end{aligned}\tag{62}$$

$$\begin{aligned}&\bar{r}_5\frac{d\bar{w}_1}{d\xi}\frac{d^2\bar{w}_2}{d\xi^2}+\bar{r}_5\frac{d\bar{w}_2}{d\xi}\frac{d^2\bar{w}_1}{d\xi^2}+\bar{r}_6\frac{d^2\bar{\theta}_3}{d\xi^2}+\bar{r}_7\frac{d^3\bar{w}_3}{d\xi^3}+\bar{r}_8\left(\bar{\theta}_3+\frac{d\bar{w}_3}{d\xi}\right)+\bar{r}_9\frac{d\bar{\phi}_3}{d\xi}+\bar{r}_{10}\frac{d\bar{\varphi}_3}{d\xi}\\&-\bar{l}^2\left[\begin{aligned}&\bar{r}_5\left(3\frac{d^3\bar{w}_1}{d\xi^3}\frac{d^2\bar{w}_2}{d\xi^2}+3\frac{d^3\bar{w}_2}{d\xi^3}\frac{d^2\bar{w}_1}{d\xi^2}+\frac{d\bar{w}_1}{d\xi}\frac{d^4\bar{w}_2}{d\xi^4}+\frac{d\bar{w}_2}{d\xi}\frac{d^4\bar{w}_1}{d\xi^4}\right)+\bar{r}_6\frac{d^4\bar{\theta}_3}{d\xi^4}+\bar{r}_7\frac{d^5\bar{w}_3}{d\xi^5}\\&+\bar{r}_8\left(\frac{d^2\bar{\theta}_3}{d\xi^2}+\frac{d^3\bar{w}_3}{d\xi^3}\right)+\bar{r}_9\frac{d^3\bar{\phi}_3}{d\xi^3}+\bar{r}_{10}\frac{d^3\bar{\varphi}_3}{d\xi^3}\end{aligned}\right]=0\end{aligned}\tag{63}$$

$$\begin{aligned}&\int_0^{\pi}\left\{\begin{aligned}&\frac{\bar{A}_{11}\pi}{2}\left(\frac{d\bar{w}_1}{d\xi}\right)^2+\bar{B}_{11}\frac{d\bar{\theta}_2}{d\xi}-\bar{c}_1\bar{E}_{11}\left(\frac{d\bar{\theta}_2}{d\xi}+\frac{d^2\bar{w}_2}{d\xi^2}\right)\\&-\bar{l}^2\left[\bar{A}_{11}\pi\left(\frac{d\bar{w}_1}{d\xi}\frac{d^3\bar{w}_1}{d\xi^3}+\frac{d^2\bar{w}_1}{d\xi^2}\frac{d^2\bar{w}_1}{d\xi^2}\right)+\bar{B}_{11}\frac{d^3\bar{\theta}_2}{d\xi^3}-\bar{c}_1\bar{E}_{11}\left(\frac{d^3\bar{\theta}_2}{d\xi^3}+\frac{d^4\bar{w}_2}{d\xi^4}\right)\right]\end{aligned}\right\}d\xi\left(\frac{d^2\bar{w}_1}{d\xi^2}-\bar{\mu}^2\frac{d^4\bar{w}_1}{d\xi^4}\right)\\&\int_0^{\pi}\left\{\bar{B}_{11}\frac{d\bar{\theta}_1}{d\xi}-\bar{c}_1\bar{E}_{11}\left(\frac{d\bar{\theta}_1}{d\xi}+\frac{d^2\bar{w}_1}{d\xi^2}\right)-\bar{l}^2\left[\bar{B}_{11}\frac{d^3\bar{\theta}_1}{d\xi^3}-\bar{c}_1\bar{E}_{11}\left(\frac{d^3\bar{\theta}_1}{d\xi^3}+\frac{d^4\bar{w}_1}{d\xi^4}\right)\right]\right\}d\xi\left(\frac{d^2\bar{w}_2}{d\xi^2}-\bar{\mu}^2\frac{d^4\bar{w}_2}{d\xi^4}\right)\\&-2(\bar{N}_E+\bar{N}_H+\bar{N}_T)\left(\frac{d^2\bar{w}_3}{d\xi^2}-\bar{\mu}^2\frac{d^4\bar{w}_3}{d\xi^4}\right)+\lambda_q^3-\frac{\bar{r}_8}{\pi}\left(\frac{d\bar{\theta}_3}{d\xi}+\frac{d^2\bar{w}_3}{d\xi^2}\right)-\frac{\bar{r}_2}{\pi^2}\frac{d^2\bar{\phi}_3}{d\xi^2}-\frac{\bar{r}_4}{\pi^2}\frac{d^2\bar{\varphi}_3}{d\xi^2}-\bar{c}_1^2\bar{H}_{11}\frac{d^4\bar{w}_3}{d\xi^4}\\&-\bar{l}^2\left[\begin{aligned}&\bar{c}_1\bar{E}_{11}\pi\left(3\frac{d^2\bar{w}_1}{d\xi^2}\frac{d^3\bar{w}_2}{d\xi^3}+3\frac{d^2\bar{w}_2}{d\xi^2}\frac{d^3\bar{w}_1}{d\xi^3}+4\frac{d^2\bar{w}_1}{d\xi^2}\frac{d^4\bar{w}_2}{d\xi^4}+4\frac{d^2\bar{w}_2}{d\xi^2}\frac{d^4\bar{w}_1}{d\xi^4}+\frac{d\bar{w}_1}{d\xi}\frac{d^5\bar{w}_2}{d\xi^5}+\frac{d\bar{w}_2}{d\xi}\frac{d^5\bar{w}_1}{d\xi^5}\right)\\&-\bar{c}_1^2\bar{H}_{11}\frac{d^6\bar{w}_3}{d\xi^6}-\frac{\bar{r}_8}{\pi}\left(\frac{d^3\bar{\theta}_3}{d\xi^3}+\frac{d^4\bar{w}_3}{d\xi^4}\right)-\frac{\bar{r}_2}{\pi^2}\frac{d^4\bar{\phi}_3}{d\xi^4}-\frac{\bar{r}_4}{\pi^2}\frac{d^4\bar{\varphi}_3}{d\xi^4}-\frac{\bar{r}_7}{\pi}\frac{d^5\bar{\theta}_3}{d\xi^5}\end{aligned}\right]\\&+\pi\bar{c}_1\bar{E}_{11}\left[\left(\frac{d^2\bar{w}_1}{d\xi^2}\frac{d^2\bar{w}_2}{d\xi^2}\right)^2+\frac{d\bar{w}_1}{d\xi}\frac{d^3\bar{w}_2}{d\xi^3}+\frac{d\bar{w}_2}{d\xi}\frac{d^3\bar{w}_1}{d\xi^3}\right]-\frac{\bar{r}_7}{\pi}\frac{d^3\bar{\theta}_3}{d\xi^3}=0\end{aligned}\tag{64}$$

4.1 For a PFGMTEEMs beam with simply supported ends

In order to solve above-derived perturbation equations, asymptotic solutions of dimensionless displacement, dimensionless rotation angle, dimensionless electric potential aligned with dimensionless magnetic potential, satisfying boundary conditions of simply supported ends, are approximated as

$$\begin{aligned}&\bar{w}(\xi)=\varepsilon A_{10}^1\sin(m\xi)+\varepsilon^3A_{10}^3\sin(3m\xi)+O(\varepsilon^4);\\&\bar{\theta}(\xi)=\varepsilon B_{10}^1\cos(m\xi)+\varepsilon^3B_{10}^3\cos(3m\xi)+O(\varepsilon^4);\\&\bar{\phi}(\xi)=\varepsilon C_{10}^1\sin(m\xi)+\varepsilon^3C_{10}^3\sin(3m\xi)+O(\varepsilon^4);\\&\bar{\varphi}(\xi)=\varepsilon D_{10}^1\sin(m\xi)+\varepsilon^3D_{10}^3\sin(3m\xi)+O(\varepsilon^4);\end{aligned}\tag{65}$$

We substitute Eq. (65) into Eqs. (53)-(55) to arrive at

$$\left(1+m^2\bar{l}^2\right)\left(B_{10}^1\bar{r}_1m+\bar{r}_2A_{10}^1m^2+C_{10}^1a_1+D_{10}^1a_2\right)=0\tag{66}$$

$$\left(1+m^2\bar{l}^2\right)\left(\bar{r}_3B_{10}^1m+\bar{r}_4A_{10}^1m^2+C_{10}^1a_2+D_{10}^1a_3\right)=0\tag{67}$$

$$\left(1+m^2\bar{l}^2\right)\left(B_{10}^1a_4+A_{10}^1a_5-\bar{r}_9C_{10}^1m-\bar{r}_{10}D_{10}^1m\right)=0\tag{68}$$

where

$$\begin{aligned}&a_1=\bar{X}_{33}+\bar{X}_{11}m^2;a_2=\bar{Y}_{33}+\bar{Y}_{11}m^2;a_3=\bar{T}_{33}+\bar{T}_{11}m^2;\\&a_4=\bar{r}_6m^2-\bar{r}_8;a_5=\bar{r}_7m^3-\bar{r}_8m;\end{aligned}$$

Via solving Eqs. (66)-(68), we get

$$B_{10}^1=\eta_1A_{10}^1;C_{10}^1=\eta_2A_{10}^1;D_{10}^1=\eta_3A_{10}^1;\tag{69}$$

in which

$$\eta_1=-\frac{a_2^2a_5-a_1a_3a_5+a_2m^3\bar{r}_{10}\bar{r}_2-a_1m^3\bar{r}_{10}\bar{r}_4-a_3m^3\bar{r}_2\bar{r}_9+a_2m^3\bar{r}_4\bar{r}_9}{a_2^2a_4-a_1a_3a_4+a_2m^2\bar{r}_{10}\bar{r}_1-a_1m^2\bar{r}_{10}\bar{r}_3-a_3m^2\bar{r}_1\bar{r}_9+a_2m^2\bar{r}_3\bar{r}_9};$$

$$\eta_2=-\frac{m\left(a_3a_5\bar{r}_1-a_2a_5\bar{r}_3-a_3a_4m\bar{r}_2+a_2a_4m\bar{r}_4+m^3\bar{r}_{10}\bar{r}_1\bar{r}_4-m^3\bar{r}_{10}\bar{r}_2\bar{r}_3\right)}{a_2^2a_4-a_1a_3a_4+a_2m^2\bar{r}_{10}\bar{r}_1-a_1m^2\bar{r}_{10}\bar{r}_3-a_3m^2\bar{r}_1\bar{r}_9+a_2m^2\bar{r}_3\bar{r}_9};$$

$$\eta_3=\frac{m\left(a_2a_5\bar{r}_1-a_1a_5\bar{r}_3-a_2a_4m\bar{r}_2+a_1a_4m\bar{r}_4+m^3\bar{r}_1\bar{r}_4\bar{r}_9-m^3\bar{r}_2\bar{r}_3\bar{r}_9\right)}{a_2^2a_4-a_1a_3a_4+a_2m^2\bar{r}_{10}\bar{r}_1-a_1m^2\bar{r}_{10}\bar{r}_3-a_3m^2\bar{r}_1\bar{r}_9+a_2m^2\bar{r}_3\bar{r}_9};$$

The substitution of Eqs. (65) and (69) into Eq. (56) yields

$$\lambda_q^1=\left[\begin{aligned}&\left(1+m^2\bar{l}^2\right)\left(\frac{\left(\eta_1\bar{r}_7m^3-\eta_1\bar{r}_8-\bar{r}_8m\right)\pi-\left(\bar{r}_2\eta_2m^2+\bar{r}_4\eta_3m^2\right)}{\pi^2}+\bar{c}_1^2\bar{H}_{11}m^4\right)\\&-2m^2(\bar{N}_E+\bar{N}_H+\bar{N}_T)\left(1+m^2\bar{\mu}^2\right)\end{aligned}\right]A_{10}^1\sin(m\xi)\tag{70}$$

By substituting Eq. (65) and Eq. (69) into Eq. (60), λ_9^2 is determined as

$$\lambda_q^2=\left\{\begin{aligned}&\left[(-1)^m-1\right]\left(1+m^2\bar{l}^2\right)\left(1+\bar{\mu}^2m^2\right)\left[\eta_1\bar{B}_{11}-\bar{c}_1\bar{E}_{11}\left(\eta_1+m\right)\right]m^2\sin(m\xi)\\&+\pi\bar{c}_1\bar{E}_{11}m^4\left(1+4m^2\bar{l}^2\right)\cos(2m\xi)\end{aligned}\right\}\left(A_{10}^1\right)^2\tag{71}$$

We substitute Eq. (65) into Eq. (61)-(63), again, obtaining

$$\left(1+9m^2\bar{l}^2\right)\left(B_{10}^3\bar{r}_13m+\bar{r}_2A_{10}^39m^2+C_{10}^3b_1+D_{10}^3b_2\right)=0\tag{72}$$

$$\left(1+9m^2\bar{l}^2\right)\left(\bar{r}_3B_{10}^33m+\bar{r}_4A_{10}^39m^2+C_{10}^3b_2+D_{10}^3b_3\right)=0\tag{73}$$

$$\left(1+9m^2\bar{l}^2\right)\left(B_{10}^3b_4+A_{10}^3b_5-\bar{r}_9C_{10}^33m-\bar{r}_{10}D_{10}^33m\right)=0\tag{74}$$

where

$$b_1 = \bar{X}_{33} + \bar{X}_{11} 9m^2; b_2 = \bar{Y}_{33} + \bar{Y}_{11} 9m^2; b_3 = \bar{T}_{33} + \bar{T}_{11} 9m^2;$$
$$b_4 = \bar{r}_6 9m^2 - \bar{r}_8; b_5 = \bar{r}_7 27m^3 - \bar{r}_8 3m;$$

Via solving Eqs. (72)-(74), we get

$$B_{10}^3 = \tau_1 A_{10}^3; C_{10}^3 = \tau_2 A_{10}^3; D_{10}^3 = \tau_3 A_{10}^3; \tag{75}$$

in which

$$\tau_1 = -\frac{b_2^2 a_5 - b_1 b_3 b_5 + 27 b_2 m^3 \bar{r}_{10} \bar{r}_2 - 27 b_1 m^3 \bar{r}_{10} \bar{r}_4 - 27 b_3 m^3 \bar{r}_2 \bar{r}_9 + 27 b_2 m^3 \bar{r}_4 \bar{r}_9}{b_2^2 b_4 - b_1 b_3 b_4 + 9 b_2 m^2 \bar{r}_{10} \bar{r}_1 - 9 b_1 m^2 \bar{r}_{10} \bar{r}_3 - 9 b_3 m^2 \bar{r}_1 \bar{r}_9 + 9 b_2 m^2 \bar{r}_3 \bar{r}_9}$$

$$\tau_2 = -\frac{3m\left(b_3 b_5 \bar{r}_1 - b_2 b_5 \bar{r}_3 - 3 b_3 b_4 m \bar{r}_2 + 3 b_2 b_4 m \bar{r}_4 + 27 m^3 \bar{r}_{10} \bar{r}_1 \bar{r}_4 - 27 m^3 \bar{r}_{10} \bar{r}_2 \bar{r}_3\right)}{b_2^2 b_4 - b_1 b_3 b_4 + 9 b_2 m^2 \bar{r}_{10} \bar{r}_1 - 9 b_1 m^2 \bar{r}_{10} \bar{r}_3 - 9 b_3 m^2 \bar{r}_1 \bar{r}_9 + 9 b_2 m^2 \bar{r}_3 \bar{r}}$$

$$\tau_3 = \frac{3m\left(b_2 b_5 \bar{r}_1 - b_1 b_5 \bar{r}_3 - 3 b_2 b_4 m \bar{r}_2 + 3 b_1 b_4 m \bar{r}_4 + 27 m^3 \bar{r}_1 \bar{r}_4 \bar{r}_9 - 27 m^3 \bar{r}_2 \bar{r}_3 \bar{r}_9\right)}{b_2^2 b_4 - b_1 b_3 b_4 + 9 b_2 m^2 \bar{r}_{10} \bar{r}_1 - 9 b_1 m^2 \bar{r}_{10} \bar{r}_3 - 9 b_3 m^2 \bar{r}_1 \bar{r}_9 + 9 b_2 m^2 \bar{r}_3 \bar{r}}$$

Then, the substitution of Eq. (65) and Eq. (75) into Eq. (64) yields

$$\begin{aligned}\lambda_q^3 = &\left(1+9m^2\bar{l}^2\right)\left[81m^4\bar{c}_1^2\bar{H}_{11} + \frac{\pi\left(27\tau_1 m^3 \bar{r}_7 - \tau_1 \bar{r}_8 - 3m\bar{r}_8\right) - 9m^2\left(\bar{r}_2\tau_2 + \bar{r}_4\tau_3\right)}{\pi^2}\right] A_{10}^3 \sin(3m\xi) \\ &+ \frac{\bar{A}_{11}\pi^2 m^4}{4}(1+m^2\bar{\mu}^2)\left(A_{10}^1\right)^3 \sin(m\xi) - 18m^2(1+9m^2\bar{\mu}^2)\left(\bar{N}_T + \bar{N}_E + \bar{N}_H\right) A_{10}^3 \sin(3m\xi)\end{aligned} \tag{76}$$

As a result, asymptotic solutions of dimensionless transverse load can be achieved as

$$\lambda_q = \lambda_q^1 + \lambda_q^2 + \lambda_q^3 + O(\varepsilon^4); \tag{77}$$

Next, two kinds of transverse loading, a uniform transverse loading and a sinusoidal transverse loading, are taken into account in the present work.

For a uniform transverse loading, the expression of dimensionless transverse load is given by

$$\lambda_q = \tilde{q}\left(\xi\right)^0 \tag{78}$$

For a sinusoidal transverse loading, the expression of dimensionless transverse load is given by

$$\lambda_q = \tilde{q}\sin\left(m\xi\right) \tag{79}$$

By employing the method of Galerkin to Eq. (77), we have

$$\int_0^\pi \left\{\begin{aligned} &\left[\begin{aligned}&\left(1+m^2\bar{l}^2\right)\left(\frac{\left(\eta_1\bar{r}_7 m^3 - \eta_1\bar{r}_8 - \bar{r}_8 m\right)\pi - \left(\bar{r}_2\eta_2 m^2 + \bar{r}_4\eta_3 m^2\right)}{\pi^2} + \bar{c}_1^2\bar{H}_{11}m^4\right) \\ &-2m^2(\bar{N}_E + \bar{N}_H + \bar{N}_T)\left(1+m^2\bar{\mu}^2\right)\end{aligned}\right] A_{10}^1 \sin(m\xi) + \\ &\left[(-1)^m - 1\right]\left(1+m^2\bar{l}^2\right)\left(1+\bar{\mu}^2 m^2\right)\left[\eta_1\bar{B}_{11} - \bar{c}_1\bar{E}_{11}\left(\eta_1 + m\right)\right] m^2 \sin(m\xi)\left(A_{10}^1\right)^2 - \lambda_q \\ &+\pi\bar{c}_1\bar{E}_{11}m^4\left(1+4m^2\bar{l}^2\right)\cos(2m\xi)\left(A_{10}^1\right)^2 \\ &+\left(1+9m^2\bar{l}^2\right)\left[81m^4\bar{c}_1^2\bar{H}_{11} + \frac{\pi\left(27\tau_1 m^3\bar{r}_7 - \tau_1\bar{r}_8 - 3m\bar{r}_8\right) - 9m^2\left(\bar{r}_2\tau_2 + \bar{r}_4\tau_3\right)}{\pi^2}\right] A_{10}^3 \sin(3m\xi) \\ &-18m^2(1+9m^2\bar{\mu}^2)\left(\bar{N}_T + \bar{N}_E + \bar{N}_H\right) A_{10}^3 \sin(3m\xi) + \frac{\bar{A}_{11}\pi^2 m^4}{4}(1+m^2\bar{\mu}^2)\left(A_{10}^1\right)^3 \sin(m\xi)\end{aligned}\right\} \sin(m\xi)\,\mathrm{d}\xi = 0 \tag{80}$$

After doing some mathematical manipulations, the two kinds of analytical solution of dimensionless transverse load can be obtained from Eq. (80).

A uniform transverse loading

$$\begin{aligned}\tilde{q} = &\frac{\pi m}{4}\left[\begin{aligned}&\left(1+m^2\bar{l}^2\right)\left(\frac{\left(\eta_1\bar{r}_7 m^3 - \eta_1\bar{r}_8 - \bar{r}_8 m\right)\pi - \left(\bar{r}_2\eta_2 m^2 + \bar{r}_4\eta_3 m^2\right)}{\pi^2} + \bar{c}_1^2\bar{H}_{11}m^4\right) \\ &-2m^2(\bar{N}_E + \bar{N}_H + \bar{N}_T)\left(1+m^2\bar{\mu}^2\right)\end{aligned}\right] A_{10}^1 + \\ &\left[(-1)^m - 1\right]\left\{\begin{aligned}&\frac{\pi m^3}{4}(1+m^2\bar{l}^2)(1+m^2\bar{\mu}^2)\left[\eta_1(\bar{B}_{11} - \bar{c}_1\bar{E}_{11}) - m\bar{c}_1\bar{E}_{11}\right] \\ &+(1+4m^2\bar{l}^2)\bar{c}_1\bar{E}_{11}\frac{\pi m^4}{6}\end{aligned}\right\}(A_{10}^1)^2 + \frac{\bar{A}_{11}\pi^3 m^5}{16}(1+m^2\bar{\mu}^2)(A_{10}^1)^3\end{aligned} \tag{81}$$

A sinusoidal transverse loading

$$\begin{aligned}\tilde{q} = &\left[\begin{aligned}&\left(1+m^2\bar{l}^2\right)\left(\frac{\left(\eta_1\bar{r}_7 m^3 - \eta_1\bar{r}_8 - \bar{r}_8 m\right)\pi - \left(\bar{r}_2\eta_2 m^2 + \bar{r}_4\eta_3 m^2\right)}{\pi^2} + \bar{c}_1^2\bar{H}_{11}m^4\right) \\ &-2m^2(\bar{N}_E + \bar{N}_H + \bar{N}_T)\left(1+m^2\bar{\mu}^2\right)\end{aligned}\right] A_{10}^1 + \\ &\left[(-1)^m - 1\right]\left\{\begin{aligned}&m^2(1+m^2\bar{l}^2)(1+m^2\bar{\mu}^2)\left[\eta_1(\bar{B}_{11} - \bar{c}_1\bar{E}_{11}) - m\bar{c}_1\bar{E}_{11}\right] \\ &+(1+4m^2\bar{l}^2)\bar{c}_1\bar{E}_{11}\frac{2m^3}{3\pi}\end{aligned}\right\}(A_{10}^1)^2 + \frac{\bar{A}_{11}\pi^2 m^4}{4}(1+m^2\bar{\mu}^2)(A_{10}^1)^3\end{aligned} \tag{82}$$

It should be pointed out that A_{10}^1 as the perturbation parameter in Eqs. (81) and (82) stands for the dimensionless maximum deflection, the value of which can be determined from the first equation of Eq. (65) when setting $\xi = \pi / 2m$.

$$A_{10}^1 = \bar{W}_m = \frac{W_m}{L}; \tag{83}$$

Consequently, the expressions of Eq. (81) and Eq. (82) can be, respectively, rewritten as

$$\begin{aligned}\frac{\tilde{q}L^2}{S\pi^2} = &\frac{\pi m}{4}\left[\begin{aligned}&\left(1+m^2\bar{l}^2\right)\left(\frac{\left(\eta_1\bar{r}_7 m^3 - \eta_1\bar{r}_8 - \bar{r}_8 m\right)\pi - \left(\bar{r}_2\eta_2 m^2 + \bar{r}_4\eta_3 m^2\right)}{\pi^2} + \bar{c}_1^2\bar{H}_{11}m^4\right) \\ &-2m^2(\bar{N}_E + \bar{N}_H + \bar{N}_T)\left(1+m^2\bar{\mu}^2\right)\end{aligned}\right]\frac{W_m}{L} + \\ &\left[(-1)^m - 1\right]\left\{\begin{aligned}&\frac{\pi m^3}{4}(1+m^2\bar{l}^2)(1+m^2\bar{\mu}^2)\left[\eta_1(\bar{B}_{11} - \bar{c}_1\bar{E}_{11}) - m\bar{c}_1\bar{E}_{11}\right] \\ &+(1+4m^2\bar{l}^2)\bar{c}_1\bar{E}_{11}\frac{\pi m^4}{6}\end{aligned}\right\}\left(\frac{W_m}{L}\right)^2 \\ &+\frac{\bar{A}_{11}\pi^3 m^5}{16}(1+m^2\bar{\mu}^2)\left(\frac{W_m}{L}\right)^3 + \ldots\end{aligned} \tag{84}$$

$$\begin{aligned}\frac{\tilde{q}L^2}{S\pi^2} = &\left[\begin{aligned}&\left(1+m^2\bar{l}^2\right)\left(\frac{\left(\eta_1\bar{r}_7 m^3 - \eta_1\bar{r}_8 - \bar{r}_8 m\right)\pi - \left(\bar{r}_2\eta_2 m^2 + \bar{r}_4\eta_3 m^2\right)}{\pi^2} + \bar{c}_1^2\bar{H}_{11}m^4\right) \\ &-2m^2(\bar{N}_E + \bar{N}_H + \bar{N}_T)\left(1+m^2\bar{\mu}^2\right)\end{aligned}\right]\frac{W_m}{L} + \\ &\left[(-1)^m - 1\right]\left\{\begin{aligned}&m^2(1+m^2\bar{l}^2)(1+m^2\bar{\mu}^2)\left[\eta_1(\bar{B}_{11} - \bar{c}_1\bar{E}_{11}) - m\bar{c}_1\bar{E}_{11}\right] \\ &+(1+4m^2\bar{l}^2)\bar{c}_1\bar{E}_{11}\frac{2m^3}{3\pi}\end{aligned}\right\}\left(\frac{W_m}{L}\right)^2 \\ &+\frac{\bar{A}_{11}\pi^2 m^4}{4}(1+m^2\bar{\mu}^2)\left(\frac{W_m}{L}\right)^3 + \ldots\end{aligned} \tag{85}$$

Besides, for static analysis of a PFGMTEEMs beam, *m* is always equal to 1.

4.2 For a PFGMTEEMs beam with immovable clamped ends

For boundary conditions of immovable clamped ends, asymptotic solutions of dimensionless displacement, dimensionless rotation angle, dimensionless electric potential aligned with dimensionless magnetic potential are approximated as

$$
\begin{aligned}
&\bar{w}(\xi)=\varepsilon A_{10}^{1}\left[1-\cos(2m\xi)\right]+\varepsilon^{3}A_{10}^{3}\left[1-\cos(6m\xi)\right]+O(\varepsilon^{4});\\
&\bar{\theta}(\xi)=\varepsilon B_{10}^{1}\sin(2m\xi)+\varepsilon^{3}B_{10}^{3}\sin(6m\xi)+O(\varepsilon^{4});\\
&\bar{\phi}(\xi)=\varepsilon C_{10}^{1}\left[1-\cos(2m\xi)\right]+\varepsilon^{3}C_{10}^{3}\left[1-\cos(6m\xi)\right]+O(\varepsilon^{4});\\
&\bar{\varphi}(\xi)=\varepsilon D_{10}^{1}\left[1-\cos(2m\xi)\right]+\varepsilon^{3}D_{10}^{3}\left[1-\cos(6m\xi)\right]+O(\varepsilon^{4});
\end{aligned}
\tag{86}
$$

We substitute Eq. (86) into Eqs. (53)-(55) to arrive at

$$(1+4m^{2}\bar{l}^{2})\left(\bar{r}_{1}B_{10}^{1}2m+\bar{r}_{2}A_{10}^{1}4m^{2}+C_{10}^{1}a_{1}+D_{10}^{1}a_{2}\right)=0; \tag{87}$$

$$(1+4m^{2}\bar{l}^{2})\left(\bar{r}_{3}B_{10}^{1}2m+\bar{r}_{4}A_{10}^{1}4m^{2}+C_{10}^{1}a_{2}+D_{10}^{1}a_{3}\right)=0; \tag{88}$$

$$(1+4m^{2}\bar{l}^{2})\left(B_{10}^{1}a_{4}+A_{10}^{1}a_{5}-\bar{r}_{9}2mC_{10}^{1}-D_{10}^{1}\bar{r}_{10}2m\right)=0; \tag{89}$$

where

$$a_{1}=\bar{X}_{33}+4m^{2}\bar{X}_{11};a_{2}=\bar{Y}_{33}+4m^{2}\bar{Y}_{11};a_{3}=\bar{T}_{33}+4m^{2}\bar{T}_{11};a_{4}=4m^{2}\bar{r}_{6}-\bar{r}_{8};a_{5}=8m^{3}\bar{r}_{7}-2m\bar{r}_{8};$$

Via solving Eqs. (87)-(89), we get

$$B_{10}^{1}=\eta_{1}A_{10}^{1};C_{10}^{1}=\eta_{2}A_{10}^{1};D_{10}^{1}=\eta_{3}A_{10}^{1}; \tag{90}$$

in which

$$\eta_{1}=-\frac{a_{2}^{2}a_{5}-a_{1}a_{3}a_{5}+8a_{2}m^{3}\bar{r}_{10}\bar{r}_{2}-8a_{1}m^{3}\bar{r}_{10}\bar{r}_{4}-8a_{3}m^{3}\bar{r}_{2}\bar{r}_{9}+8a_{2}m^{3}\bar{r}_{4}\bar{r}_{9}}{a_{2}^{2}a_{4}-a_{1}a_{3}a_{4}+4a_{2}m^{2}\bar{r}_{10}\bar{r}_{1}-4a_{1}m^{2}\bar{r}_{10}\bar{r}_{3}-4a_{3}m^{2}\bar{r}_{1}\bar{r}_{9}+4a_{2}m^{2}\bar{r}_{3}\bar{r}_{9}}$$

$$\eta_{2}=-\frac{2m\left(a_{3}a_{5}\bar{r}_{1}-a_{2}a_{5}\bar{r}_{3}-2a_{3}a_{4}m\bar{r}_{2}+2a_{2}a_{4}m\bar{r}_{4}+8m^{3}\bar{r}_{10}\bar{r}_{1}\bar{r}_{4}-8m^{3}\bar{r}_{10}\bar{r}_{2}\bar{r}_{3}\right)}{a_{2}^{2}a_{4}-a_{1}a_{3}a_{4}+4a_{2}m^{2}\bar{r}_{10}\bar{r}_{1}-4a_{1}m^{2}\bar{r}_{10}\bar{r}_{3}-4a_{3}m^{2}\bar{r}_{1}\bar{r}_{9}+4a_{2}m^{2}\bar{r}_{3}\bar{r}_{9}}$$

$$\eta_{3}=\frac{2m\left(a_{2}a_{5}\bar{r}_{1}-a_{1}a_{5}\bar{r}_{3}-2a_{2}a_{4}m\bar{r}_{2}+2a_{1}a_{4}m\bar{r}_{4}+8m^{3}\bar{r}_{1}\bar{r}_{4}\bar{r}_{9}-8m^{3}\bar{r}_{2}\bar{r}_{3}\bar{r}_{9}\right)}{a_{2}^{2}a_{4}-a_{1}a_{3}a_{4}+4a_{2}m^{2}\bar{r}_{10}\bar{r}_{1}-4a_{1}m^{2}\bar{r}_{10}\bar{r}_{3}-4a_{3}m^{2}\bar{r}_{1}\bar{r}_{9}+4a_{2}m^{2}\bar{r}_{3}\bar{r}_{9}}$$

The substitution of Eq. (86) and Eq. (90) into Eq. (56) yields

$$\lambda_{q}^{1}=\left[\begin{array}{l}\left(1+4m^{2}\bar{l}^{2}\right)\left(\dfrac{\pi\eta_{1}\left(2m\bar{r}_{8}-\bar{r}_{7}8m^{3}\right)-4m^{2}\left(\bar{r}_{2}\eta_{2}+\bar{r}_{4}\eta_{3}\right)+4m^{2}\pi\bar{r}_{8}}{\pi^{2}}-\bar{c}_{1}^{2}\bar{H}_{11}16m^{4}\right)\\+8m^{2}(\bar{N}_{E}+\bar{N}_{H}+\bar{N}_{T})\left(1+4m^{2}\bar{\mu}^{2}\right)\end{array}\right]A_{10}^{1}\cos(2m\xi) \tag{91}$$

By substituting Eqs. (82) and (86) into Eq. (60), λ_{9}^{2} is determined as

$$\lambda_{q}^{2}=-\pi\bar{c}_{1}\bar{E}_{11}16m^{4}(1+16m^{2}\bar{l}^{2})(A_{10}^{1})^{2}\cos(4m\xi); \tag{92}$$

We substitute Eq. (86) into Eqs. (61)-(63), then doing some mathematical manipulations, obtaining

$$(1+36m^{2}\bar{l}^{2})\left(\bar{r}_{1}B_{10}^{3}6m+\bar{r}_{2}A_{10}^{3}36m^{2}+C_{10}^{3}b_{1}+D_{10}^{3}b_{2}\right)=0; \tag{93}$$

$$(1+36m^{2}\bar{l}^{2})\left(\bar{r}_{3}B_{10}^{3}6m+\bar{r}_{4}A_{10}^{3}36m^{2}+C_{10}^{3}b_{2}+D_{10}^{3}b_{3}\right)=0; \tag{94}$$

$$(1+36m^{2}\bar{l}^{2})\left(B_{10}^{3}b_{4}+A_{10}^{3}b_{5}-\bar{r}_{9}6mC_{10}^{3}-D_{10}^{3}\bar{r}_{10}6m\right)=0; \tag{95}$$

where

$$b_{1}=\bar{X}_{33}+\bar{X}_{11}36m^{2};b_{2}=\bar{Y}_{33}+\bar{Y}_{11}36m^{2};b_{3}=\bar{T}_{33}+\bar{T}_{11}36m^{2};b_{4}=\bar{r}_{6}36m^{2}-\bar{r}_{8};b_{5}=\bar{r}_{7}216m^{3}-\bar{r}_{8}6m;$$

Via solving Eqs. (93)-(95), we get

$$B_{10}^{3}=\tau_{1}A_{10}^{3};C_{10}^{3}=\tau_{2}A_{10}^{3};D_{10}^{3}=\tau_{3}A_{10}^{3}; \tag{96}$$

in which

$$\tau_{1}=-\frac{b_{2}^{2}b_{5}-b_{1}b_{3}b_{5}+216b_{2}m^{3}\bar{r}_{10}\bar{r}_{2}-216b_{1}m^{3}\bar{r}_{10}\bar{r}_{4}-216b_{3}m^{3}\bar{r}_{2}\bar{r}_{9}+216b_{2}m^{3}\bar{r}_{4}\bar{r}_{9}}{b_{2}^{2}b_{4}-b_{1}b_{3}b_{4}+36b_{2}m^{2}\bar{r}_{10}\bar{r}_{1}-36b_{1}m^{2}\bar{r}_{10}\bar{r}_{3}-36b_{3}m^{2}\bar{r}_{1}\bar{r}_{9}+36b_{2}m^{2}\bar{r}_{3}\bar{r}_{9}}$$

$$\tau_{2}=-\frac{6m\left(b_{3}b_{5}\bar{r}_{1}-b_{2}b_{5}\bar{r}_{3}-6b_{3}b_{4}m\bar{r}_{2}+6b_{2}b_{4}m\bar{r}_{4}+216m^{3}\bar{r}_{10}\bar{r}_{1}\bar{r}_{4}-216m^{3}\bar{r}_{10}\bar{r}_{2}\bar{r}_{3}\right)}{b_{2}^{2}b_{4}-b_{1}b_{3}b_{4}+36b_{2}m^{2}\bar{r}_{10}\bar{r}_{1}-36b_{1}m^{2}\bar{r}_{10}\bar{r}_{3}-36b_{3}m^{2}\bar{r}_{1}\bar{r}_{9}+36b_{2}m^{2}\bar{r}_{3}\bar{r}_{9}}$$

$$\tau_{3}=\frac{6m\left(b_{2}b_{5}\bar{r}_{1}-b_{1}b_{5}\bar{r}_{3}-6b_{2}b_{4}m\bar{r}_{2}+6b_{1}b_{4}m\bar{r}_{4}+216m^{3}\bar{r}_{1}\bar{r}_{4}\bar{r}_{9}-216m^{3}\bar{r}_{2}\bar{r}_{3}\bar{r}_{9}\right)}{b_{2}^{2}b_{4}-b_{1}b_{3}b_{4}+36b_{2}m^{2}\bar{r}_{10}\bar{r}_{1}-36b_{1}m^{2}\bar{r}_{10}\bar{r}_{3}-36b_{3}m^{2}\bar{r}_{1}\bar{r}_{9}+36b_{2}m^{2}\bar{r}_{3}\bar{r}_{99}}$$

Then, the substitution of Eqs. (86) and (96) into Eq. (64) yields

$$
\begin{aligned}
\lambda_{q}^{3}=&-\bar{A}_{11}4m^{4}\pi(1+4m^{2}\bar{\mu}^{2})(A_{10}^{1})^{3}\cos(2m\xi)+72m^{2}(1+36m^{2}\bar{\mu}^{2})(\bar{N}_{E}+\bar{N}_{H}+\bar{N}_{T})A_{10}^{3}\cos(6m\xi)\\
&+(1+36m^{2}\bar{l}^{2})\left[\frac{\bar{r}_{8}\left(\tau_{1}6m+36m^{2}\right)-\bar{r}_{7}\tau_{1}216m^{3}}{\pi}+\frac{36m^{2}\left(\bar{r}_{2}+\bar{r}_{4}\tau_{3}\right)}{\pi^{2}}-\bar{c}_{1}^{2}\bar{H}_{11}1296m^{4}\bar{c}_{1}^{2}\bar{H}_{11}\right]\cos(6m\xi)
\end{aligned}
\tag{97}
$$

As a result, asymptotic solutions of dimensionless transverse load can be achieved as

$$\lambda_{q}=\lambda_{q}^{1}+\lambda_{q}^{2}+\lambda_{q}^{3}+O(\varepsilon^{4}); \tag{98}$$

Similarly, two kinds of transverse loading, a uniform transverse loading and a sinusoidal transverse loading, are taken into account in the present work.

For a uniform transverse loading, the expression of dimensionless transverse load is given by

$$\lambda_{q}=\tilde{q}\left(\xi\right)^{0} \tag{99}$$

For a sinusoidal transverse loading, the expression of dimensionless transverse load is given by

$$\lambda_{q}=\tilde{q}\sin\left(m\xi\right) \tag{100}$$

By employing the method of Galerkin to Eq. (98), we have

$$\int_{0}^{\pi}\left\{\begin{array}{l}\left[\begin{array}{l}\left(1+4m^{2}\bar{l}^{2}\right)\left(\begin{array}{l}\dfrac{\pi\eta_{1}\left(2m\bar{r}_{8}-\bar{r}_{7}8m^{3}\right)-4m^{2}\left(\bar{r}_{2}\eta_{2}+\bar{r}_{4}\eta_{3}\right)+4m^{2}\pi\bar{r}_{8}}{\pi^{2}}\\-\bar{c}_{1}^{2}\bar{H}_{11}16m^{4}\end{array}\right)\\+8m^{2}(\bar{N}_{E}+\bar{N}_{H}+\bar{N}_{T})\left(1+4m^{2}\bar{\mu}^{2}\right)\end{array}\right]A_{10}^{1}\cos(2m\xi)\\+72m^{2}(1+36m^{2}\bar{\mu}^{2})(\bar{N}_{E}+\bar{N}_{H}+\bar{N}_{T})A_{10}^{3}\cos(6m\xi)\\-\bar{A}_{11}4m^{4}\pi(1+4m^{2}\bar{\mu}^{2})(A_{10}^{1})^{3}\cos(2m\xi)\\+(1+36m^{2}\bar{l}^{2})\left[\begin{array}{l}\dfrac{\bar{r}_{8}\left(\tau_{1}6m+36m^{2}\right)-\bar{r}_{7}\tau_{1}216m^{3}}{\pi}+\dfrac{36m^{2}\left(\bar{r}_{2}+\bar{r}_{4}\tau_{3}\right)}{\pi^{2}}\\-\bar{c}_{1}^{2}\bar{H}_{11}1296m^{4}\bar{c}_{1}^{2}\bar{H}_{11}\end{array}\right]\cos(6m\xi)\\-\pi\bar{c}_{1}\bar{E}_{11}16m^{4}(1+16m^{2}\bar{l}^{2})(A_{10}^{1})^{2}\cos(4m\xi)-\lambda_{q}\end{array}\right\}d\xi\left[1-\cos(2m\xi)\right]=0 \tag{101}$$

After doing some mathematical manipulations, the two analytical solutions of dimensionless transverse load can be obtained from Eq. (101).

A uniform transverse loading

$$\tilde{q}=\left[\begin{array}{l}\left(1+4m^2\bar{l}^2\right)\left(\begin{array}{c}\dfrac{2m^2\left(\bar{r}_2\eta_2+\bar{r}_4\eta_3\right)-\pi\eta_1\left(m\bar{r}_8-\bar{r}_7 4m^3\right)-2m^2\pi\bar{r}_8}{\pi^2}\\+\bar{c}_1^2\bar{H}_{11}8m^4\end{array}\right)\\-4m^2(\bar{N}_E+\bar{N}_H+\bar{N}_T)\left(1+4m^2\bar{\mu}^2\right)\end{array}\right]A_{10}^1 \quad (102)$$
$$+\bar{A}_{11}2m^4\pi(1+4m^2\bar{\mu}^2)(A_{10}^1)^3$$

A sinusoidal transverse loading

$$\tilde{q}=\frac{3m\pi}{8}\left[\begin{array}{l}\left(1+4m^2\bar{l}^2\right)\left(\begin{array}{c}\dfrac{2m^2\left(\bar{r}_2\eta_2+\bar{r}_4\eta_3\right)-\pi\eta_1\left(m\bar{r}_8-\bar{r}_7 4m^3\right)-2m^2\pi\bar{r}_8}{\pi^2}\\+\bar{c}_1^2\bar{H}_{11}8m^4\end{array}\right)\\-4m^2(\bar{N}_E+\bar{N}_H+\bar{N}_T)\left(1+4m^2\bar{\mu}^2\right)\end{array}\right]A_{10}^1 \quad (103)$$
$$+\bar{A}_{11}\frac{3}{4}m^5\pi^2(1+4m^2\bar{\mu}^2)(A_{10}^1)^3$$

It should be pointed out that A_{10}^1 as the perturbation parameter in Eqs. (102) and (103) stands for the dimensionless maximum deflection, the value of which can be determined from the first equation of Eq. (86) when setting $\xi=\pi/2m$.

$$A_{10}^1=\bar{W}_m=\frac{W_m}{2L}; \quad (104)$$

Consequently, the expressions of Eq. (102) and (103) can be, respectively, rewritten as

$$\tilde{q}=\frac{3m\pi}{8}\left[\begin{array}{l}\left(1+4m^2\bar{l}^2\right)\left(\begin{array}{c}\dfrac{2m^2\left(\bar{r}_2\eta_2+\bar{r}_4\eta_3\right)-\pi\eta_1\left(m\bar{r}_8-\bar{r}_7 4m^3\right)-2m^2\pi\bar{r}_8}{\pi^2}\\+\bar{c}_1^2\bar{H}_{11}8m^4\end{array}\right)\\-4m^2(\bar{N}_E+\bar{N}_H+\bar{N}_T)\left(1+4m^2\bar{\mu}^2\right)\end{array}\right]\left(\frac{W_m}{2L}\right) \quad (105)$$
$$+\bar{A}_{11}\frac{3}{4}m^5\pi^2(1+4m^2\bar{\mu}^2)\left(\frac{W_m}{2L}\right)^3+\ldots$$

$$\frac{\tilde{q}L^2}{S\pi^2}=\left[\begin{array}{l}\left(1+4m^2\bar{l}^2\right)\left(\begin{array}{c}\dfrac{\pi\eta_1\left(m\bar{r}_8-\bar{r}_7 4m^3\right)-2m^2\left(\bar{r}_2\eta_2+\bar{r}_4\eta_3\right)+2m^2\pi\bar{r}_8}{\pi^2}\\-\bar{c}_1^2\bar{H}_{11}8m^4\end{array}\right)\\-4m^2(\bar{N}_E+\bar{N}_H+\bar{N}_T)\left(1+4m^2\bar{\mu}^2\right)\end{array}\right]\left(\frac{W_m}{2L}\right) \quad (106)$$
$$+\bar{A}_{11}2m^4\pi(1+4m^2\bar{\mu}^2)\left(\frac{W_m}{2L}\right)^3+\ldots$$

Besides, for static analysis of a PFGMTEEMs beam, m is always equal to 1.

5. Results and discussion

In the following section, authors use the above-derived analytical solutions to conduct a comprehensive analysis of the bending behaviors for the beams made of PFGMTEEMs. The results revealed in such work will be immensely useful to others in conducting relevant researches.

5.1 Validation research

To begin with, a comparison with work of other researchers is performed by authors, the purpose of which is to validate the present analysis. Through a detailed literature review, there is no published data on static analysis of a functionally graded nanobeam subjected to multiple physical loads. So, as presented in Fig. 3, a functionally graded beam made of Si_3N_4 and SUS304 is studied by the present analytical model where a beam with L = 30h, T = 300K, E_0 = 201.04×10^{+9} is subjected to simply supported ends. It is indicated from this figure that the results predicted by the present analysis show a good agreement with the results reported by Zhang (2013), which totally manifests that the present analysis is reasonable and reliable.

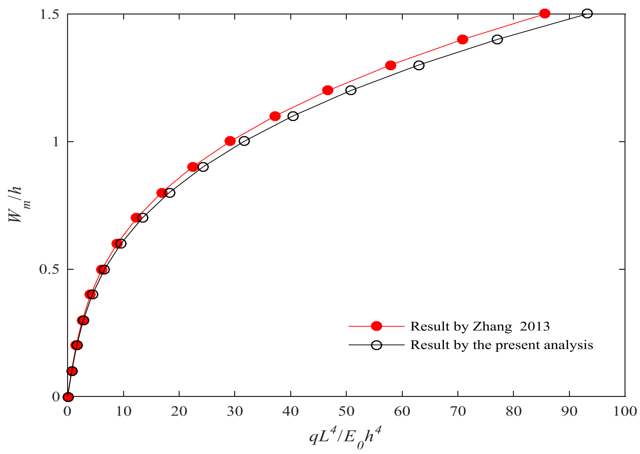

Fig. 3 Comparison of nonlinear bending of Si_3N_4/SUS304 FG beams with simply supported ends between ours and Zhang (2013)

5.2 Parametric studies

Next, a parametric analysis is carried out in detail. Here, the dimensionless load F shall be equivalent to $\tilde{q}L^4/(E_0I)$ where E_0 = 286×10^{+9} and $I=\int_A z^2\mathrm{d}A$, unless otherwise

Table 2 Magneto-electro-thermo-elastic coefficients (Ebrahimi and Barati 2016a, b)

Properties	$BaTiO_3$	$CoFe_2O_4$
C_{11} (GPa)	166	286
C_{55} (GPa)	43	45.3
e_{31} (Cm^{-2})	-4.4	0
e_{15} (Cm^{-2})	11.6	0
q_{31} (N/A m)	0	580.3
q_{15} (N/A m)	0	550
s_{11} ($10^{-9}C^2m^{-2}N^{-1}$)	11.2	0.08
s_{33} ($10^{-9}C^2m^{-2}N^{-1}$)	12.6	0.093
χ_{11} ($10^{-6}Ns^2C^{-2}/2$)	5	-590
χ_{33} ($10^{-6}Ns^2C^{-2}/2$)	10	157
$d_{11}=d_{33}$	0	0
α (10^{-6}1/K)	15.7	10
k (w/mk)	3.2	2.5
P (kgm^{-3})	5800	5300

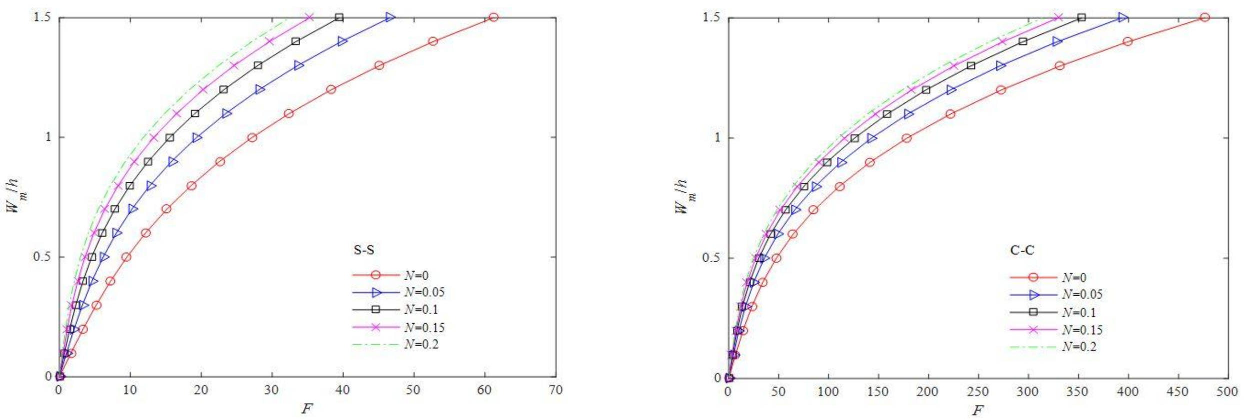

(a) Simply supported ends (b) Immovable clamped ends

Fig. 4 The effect of volume fraction index N on nonlinear bending of PFGMTEEMs beams

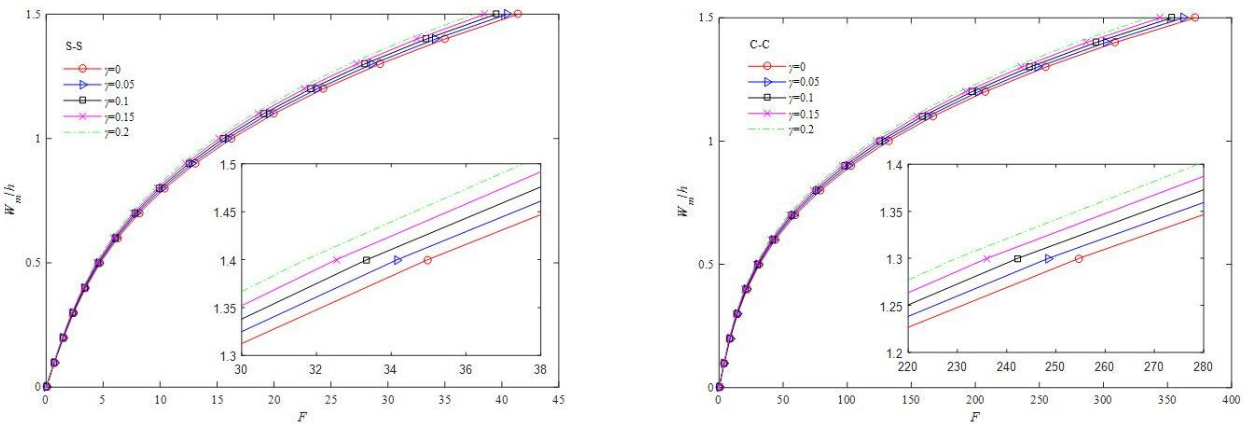

(a) Simply supported ends (b) Immovable clamped ends

Fig. 5 The effect of porosity volume fraction γ on nonlinear bending of PFGMTEEMs beams

specified. The material properties for $BaTiO_3$ and $CoFe_2O_4$ are listed in Table 2.

Figs. 4(a)-(b) respectively present the effect of volume fraction index N on nonlinear bending of PFGMTEEMs beams subjected to simply supported ends and immovable clamped ends under uniform transverse loading where h = 20 nm, $b = h$, μ = 1 nm, l = 2 nm, L = 20 h, γ = 0.1, T = 350 K, V_0 = 0.5 v, Ω = 0.02 A. It can be seen from both figures that the deflection of beams is steadily growing greater with the value of N becoming larger and larger. The reason is that the increase of N can result in the reduction in the value of total stiffness of beams. However, the difference between both figures is that the deflection of beams with simply supported ends is significantly larger than that with immovable clamped ends. That is because that as shown in Eqs. (50)-(51), for simply supported ends, the displacement and bending moment are constrained, but for clamped ends, both the displacement and the rotation angle are constrained. Thus, a conclusion can be drawn that when the stiffness of higher order boundary conditions becomes large, the deflection of beams is getting small.

Figs. 5(a)-(b) respectively display the effect of porosity volume fraction γ on nonlinear bending of PFGMTEEMs beams subjected to simply supported ends and immovable clamped ends under uniform transverse loading in which h = 20 nm, $b = h$, μ = 1 nm, l = 2 nm, L = 20 h, N = 1, T = 350 K, V_0 = 0.5 v, Ω = 0.02 A. It is indicated from these curves that whatever boundary conditions a beam is subjected to, the deflection of beams always increases with the increment of porosity volume fraction, partly because as average porosity volume fraction is increased the stiffness of beams is going to decrease.

Figs. 6(a)-(b) show the comparison of functionally graded beams subjected to different types of porosity distribution on nonlinear bending for beams with simply supported ends and immovable clamped ends under uniform transverse loading in which h = 20 nm, $b = h$, μ = 1 nm, l = 2 nm, L = 20 h, N = 1, T = 350 K, V_0 = 0.5 v, Ω = 0.02 A. It is observed from both figures that the deflection of beams subjected to the present porosity distribution is obviously smaller than that subjected to the conventional porosity distribution when both types of porosity volume fraction γ are taken at the same value. From the perspective of common fabrication methods of FGMs, a porous beam has porosities spreading through the thickness due to defect during production, which is a random process. To be specific, owing to the effective material properties of FG beams being changed along the thickness, the material

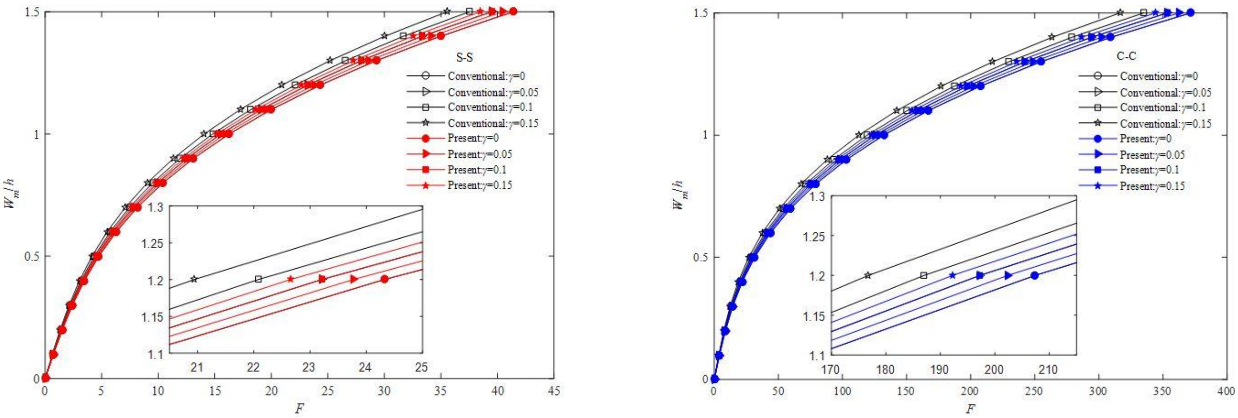

(a) Simply supported ends (b) Immovable clamped ends

Fig. 6 Comparison of functionally graded beams subjected to different types of porosity distribution on nonlinear bending

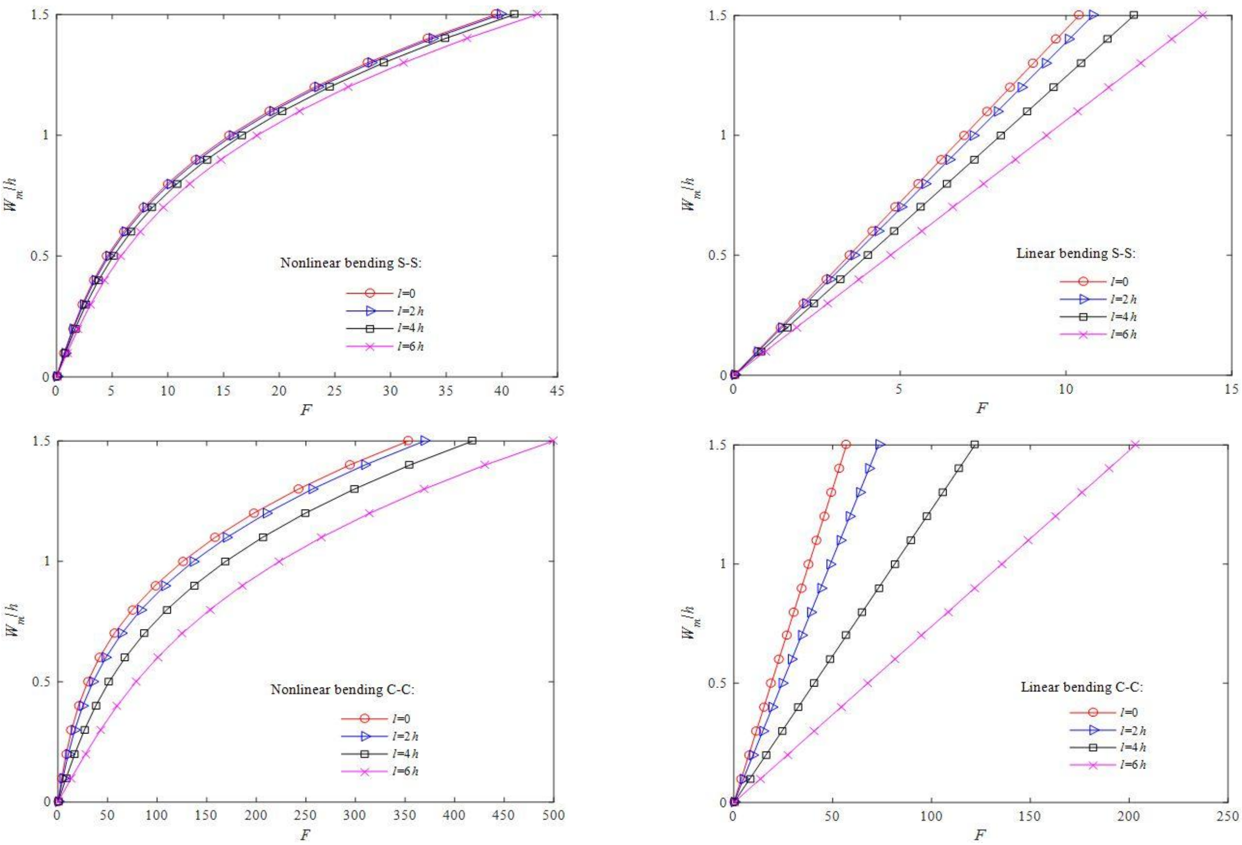

Fig. 7 The effect of strain gradient parameter l on linear and nonlinear bending of PFGMTEEMs beams with different types of boundary conditions

properties occupied by porosity are all different at different values of z. Nevertheless, as shown in Eq. (7), the material properties occupied by porosity are always equivalent to the average value of two materials in the conventional even porosity distribution. Consequently, the present even porosity distribution is much more suitable to the actual porosity distribution, which is better than the conventional.

Fig. 7 presents the effect of strain gradient parameter l on linear and nonlinear bending of PFGMTEEMs beams under uniform transverse loading with different types of boundary conditions in which h = 20 nm, $b = h$, $\mu = 0$, γ = 0.1, $L = 20\ h$, $N = 1$, T = 350 K, V_0 = 0.5 v, Ω = 0.02 A. As shown in the figure, the dimensionless deflection of the beam always decreases with the increase of strain gradient parameter l, regardless of which type of boundary conditions we choose. However, differing from linear bending, the correlation between the dimensionless deflection of the beam and the dimensionless load presents a obvious nonlinear variation for nonlinear bending. Also, within the framework of the nonlinear theory, the load-carrying capacity of beams can be improved, prominently. Therefore, for the problem of large deflection, it is not

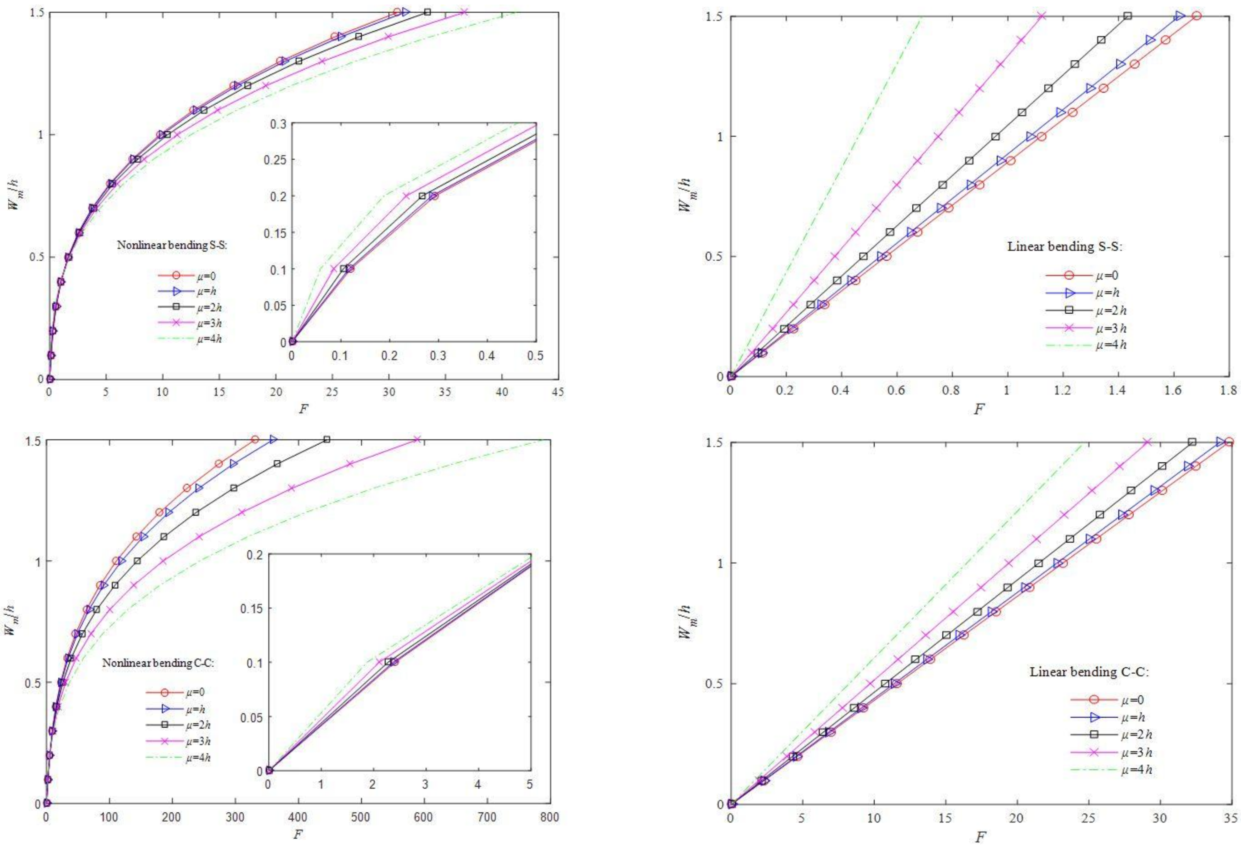

Fig. 8 The effect of nonlocal parameter μ on linear and nonlinear bending of PFGMTEEMs beams with different types of boundary conditions

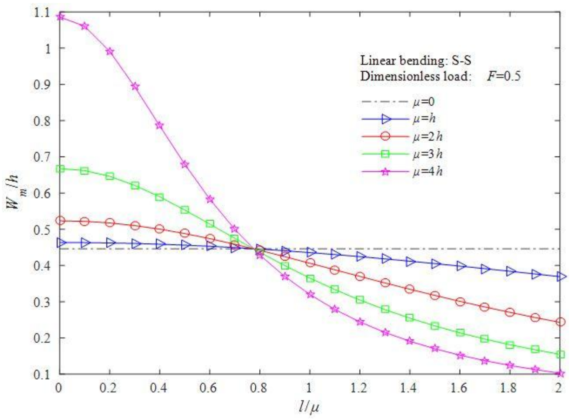

(a) The beam under dimensionless transverse load F = 0.5

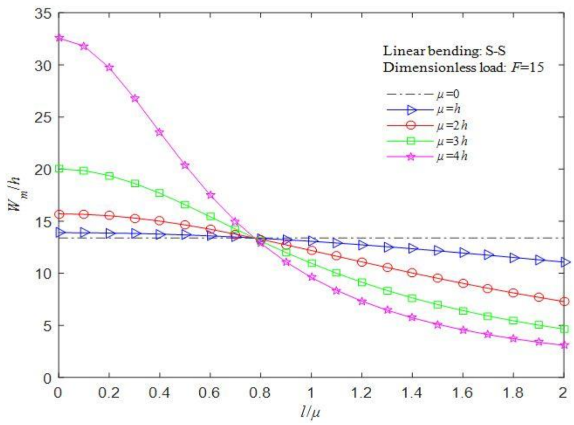

(b) The beam under dimensionless transverse load F = 15

Fig. 9 Variation of the dimensionless linear bending relevant to l/μ for the beams with simply supported ends

advise to choose linear theory to undertake the analysis, partly because the deflection of beams should not rise, infinitely, when the transverse load is large enough.

Fig. 8 shows the effect of nonlocal parameter μ on linear and nonlinear bending of PFGMTEEMs beams under uniform transverse loading with different types of boundary conditions, where h = 20 nm, b = h, l = 0, L = 20 h, γ = 0.1, N = 1, T = 350 K, V_0 = 0 v, Ω = 0 A. As vividly illustrated in this figure, for a small transverse load, the dimensionless deflection of beams can be increased with the nonlocal parameter μ becoming larger and larger, while for a considerable transverse load, the dimensionless deflection of beams can be reduced with the nonlocal parameter μ becoming larger and larger. The opposite trend is exhibited clearly in nonlinear bending whatever boundary conditions the beams are subjected to. The reason is that the nonlocal parameter μ has a direct influence on the transverse load rather than the effective stiffness of beams. This similar phenomenon can also be observed in Li *et al*. (2017) where bending of axially functionally graded beam was analyzed by using nonlocal strain gradient theory. It means that the nonlocal effect of static bending deformation is not only

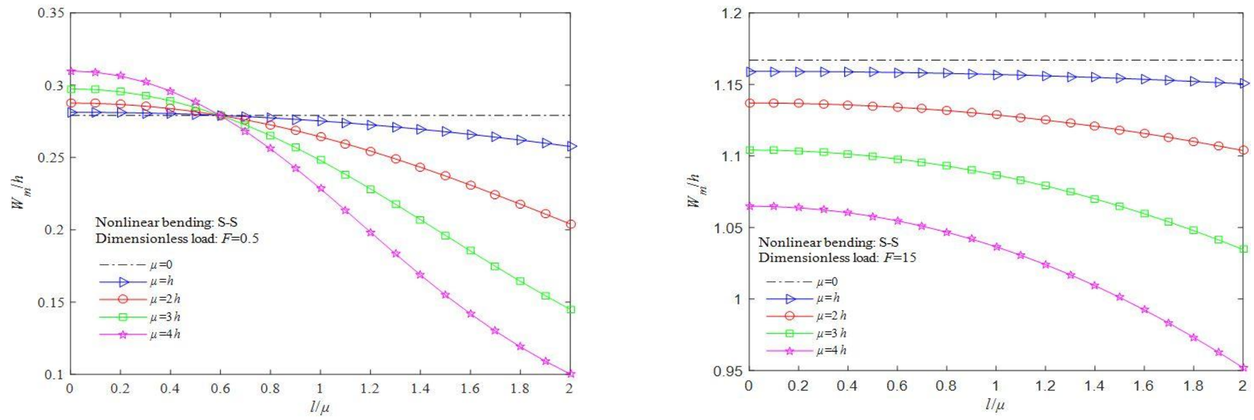

(a) The beam under dimensionless transverse load F = 0.5 (b) The beam under dimensionless transverse load F = 15

Fig. 10 Variation of the dimensionless nonlinear bending relevant to l/μ for the beam with simply supported ends

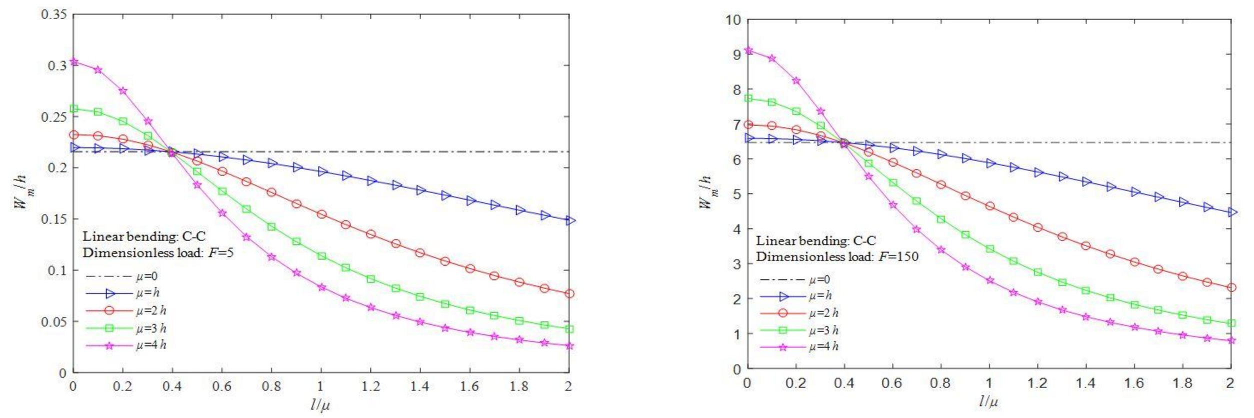

(a) The beam under dimensionless transverse load F = 0.5 (b) The beam under dimensionless transverse load F = 150

Fig. 11 Variation of the dimensionless linear bending relevant to l/μ for the beams with immovable clamped ends

dependent on nonlocal parameter μ but also influenced by distributed transverse load.

Figs. 9(a)-(b) reflects variation of the dimensionless linear bending relevant to l/μ for the beam under uniform transverse loading with simply supported ends where h = 20 nm, $b = h$, l = 0, L = 20 h, γ = 0.1, N = 1, T = 350 K, V_0 = 0 v, Ω = 0 A. From this figure, we can know that when l/μ >1, the dimensionless deflection obtained by nonlocal strain gradient theory is smaller than that obtained by classical elasticity theory and the dimensionless deflection can be decreased with the increment of nonlocal parameter μ; when l/μ = 1, the dimensionless deflection obtained by nonlocal strain gradient theory is equal to that obtained by classical elasticity theory; when l/μ < 1, the dimensionless deflection obtained by nonlocal strain gradient theory is larger than that obtained by classical elasticity theory and the dimensionless deflection can be increased with the increment of nonlocal parameter μ. From the perspective of the effective stiffness, that is because that the effect of stiffness-softening is greater than the effect of stiffness-hardening on the dimensionless deflection at a relatively smaller parameter l, however, is smaller than the effect of stiffness-hardening on the dimensionless deflection at a relatively bigger parameter l; both types of the effective stiffness variation cancel each other out with the result of parameter μ equivalent to the result of parameter l. Furthermore, through comparing Figs. 9(a) and (b), we have a good knowledge that the dimensionless deflection of beams under dimensionless transverse load F = 15 is distinctly larger than that under dimensionless transverse load F = 0.5.

Fig. 10 reflects variation of the dimensionless nonlinear bending relevant to l/μ for the beam under uniform transverse loading with simply supported ends in which h = 20 nm, $b = h$, l = 0, L = 20 h, γ = 0.1, N = 1, T = 350 K, V_0 = 0 v, Ω = 0 A. It can be seen from Fig. 10(c) that the variation of the dimensionless nonlinear bending is similar to the variation of the dimensionless linear bending when a beam is subjected to dimensionless transverse load F = 0.5. Nevertheless, when a beam is subjected to dimensionless transverse load F = 15, as presented in Fig. 10(d), the dimensionless deflection obtained by nonlocal strain gradient theory is always smaller than that obtained by classical elasticity theory. That is due to the fact that for a nan-structure subjected to a big transverse load, the nonlocal effect is mainly influenced by the distributed external load rather than the effective stiffness of structure.

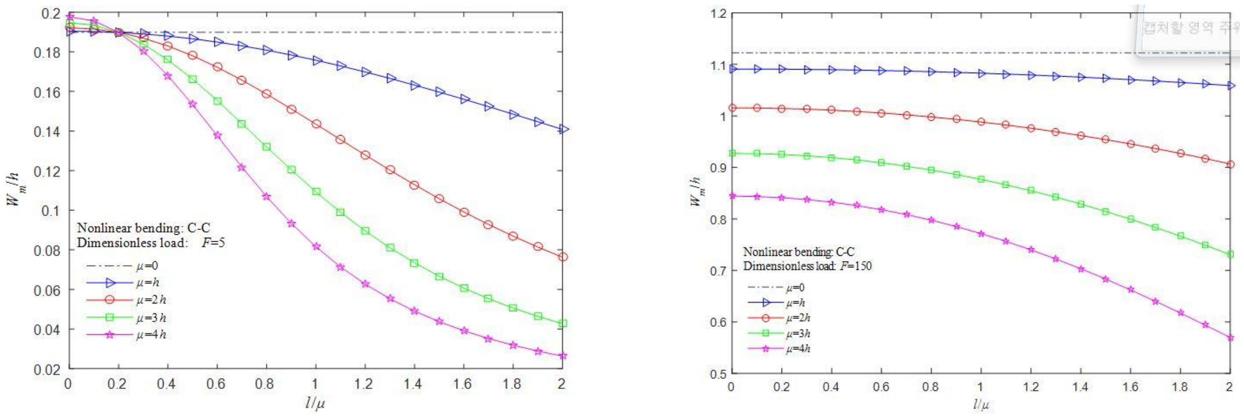

(a) The beam under dimensionless transverse load $F = 0.5$ (b) The beam under dimensionless transverse load $F = 150$

Fig. 12 Variation of the dimensionless nonlinear bending relevant to l/μ for the beam with immovable clamped ends

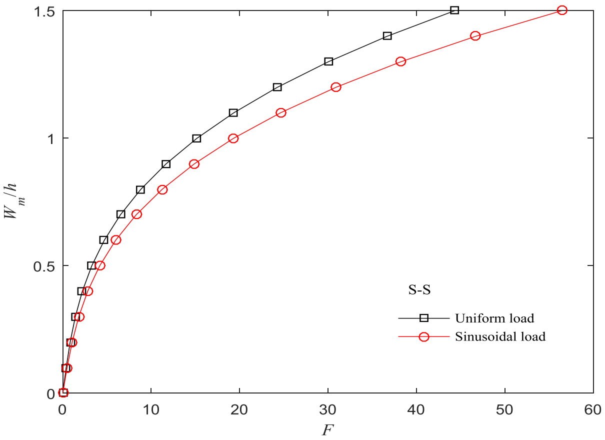

Fig. 13 The effect of two kinds of transverse loading on the nonlinear bending of PFGMTEEMs beams with simply supported ends

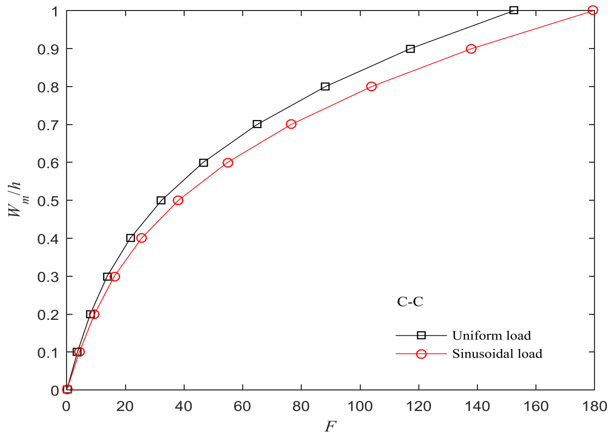

Fig. 14 The effect of two kinds of transverse loading on the nonlinear bending of PFGMTEEMs beams with immovable clamped ends

Figs. 11(a)-(b) and Figs. 12(c)-(d) reflect the variation of the dimensionless linear bending relevant to l/μ for the beam with immovable clamped ends and the variation of the dimensionless nonlinear bending relevant to l/μ for the beam under uniform transverse loading with immovable clamped ends, respectively. The conclusions can be drawn from these curves that the phenomena observed in analysis of beams with simply supported ends can also be observed in analysis of beams with immovable clamped ends, and the laws of nonlocal parameter, strain gradient parameter and the ratio of strain gradient parameter to nonlocal parameter related to beams subjected to simply supported ends are also appropriated for beams subjected to immovable clamped ends.

In Figs. 13-14, the effect of two kinds of transverse loading on the nonlinear bending of PFGMTEEMs beams with different boundary conditions are plotted where $h = 20$ nm, $b = h$, $\mu = 1$ nm, $l = 2$ nm, $L = 15\,h$, $\gamma = 0.1$, $N = 1$, $V_0 = 0$ v, $\Omega = 0$ A, $T = 300$ K. It can be seen that the load-deflection curves of PFGMTEEMs beams subjected to a sinusoidal load are lower than those of the same beams subjected to a uniform load. That is because the resultant force of the uniform transverse load is larger than that of the sinusoidal transverse load at the same conditions.

In Figs. 15-16, the effect of dimensionless temperature on the nonlinear bending of PFGMTEEMs beams under uniform transverse loading with different boundary conditions are plotted where $h = 20$ nm, $b = h$, $\mu = 1$ nm, $l = 2$ nm, $L = 15\,h$, $\gamma = 0.1$, $N = 1$, $V_0 = 0$ v, $\Omega = 0$ A. We can see that as the dimensionless temperature continues to rise, the deflection of PFGMTEEMs beams becomes large, no matter which type of boundary conditions a beam is subjected to. That is because the total stiffness of beams is reduced by the rise of dimensionless temperature.

The effect of external electric voltages on the nonlinear bending of PFGMTEEMs beams under uniform transverse loading with simply supported ends and immovable clamped ends are shown in Figs. 17 and 18, where $h = 20$ nm, $b = h$, $\mu = 1$ nm, $l = 2$ nm, $L = 15\,h$, $\gamma = 0.1$, $N = 1$, $T = 300$ K, $\Omega = 0$ A. As is indicated in both figures, the deflection of beams is steadily growing considerable when the external electric voltage increasing continuously. That is due to the fact compressive forces are produced by applying positive voltages while tensile forces are produced by applying negative voltages.

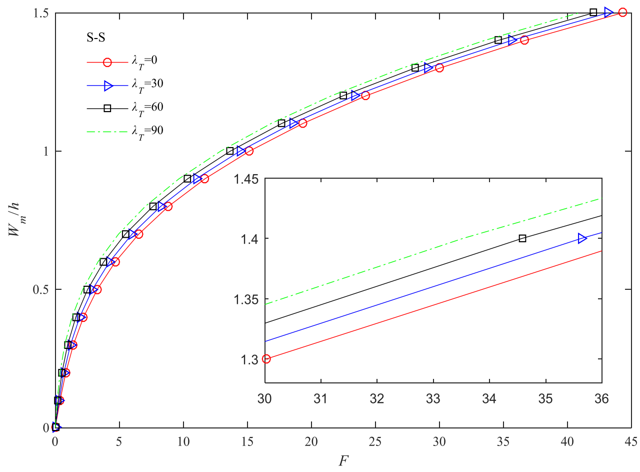

Fig. 15 The effect of dimensionless temperature on the nonlinear bending of PFGMTEEMs beams with simply supported ends

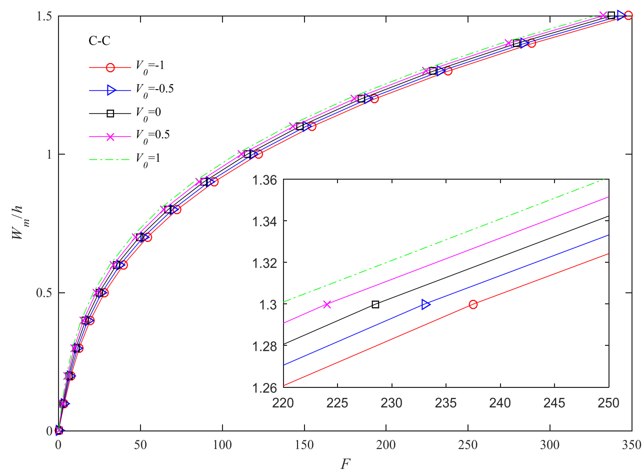

Fig. 18 The effect of external electric voltages on the nonlinear bending of PFGMTEEMs beams with immovable clamped ends

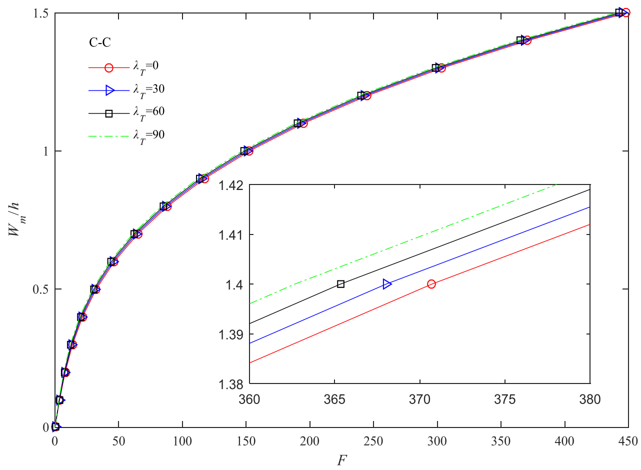

Fig. 16 The effect of dimensionless temperature on the nonlinear bending of PFGMTEEMs beams with immovable clamped ends

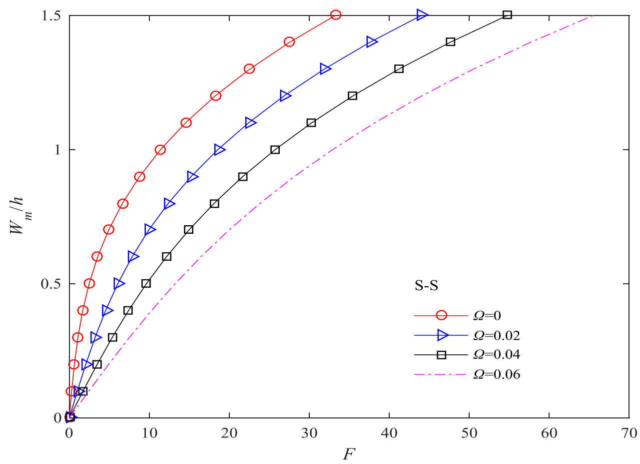

Fig. 19 The effect of initial magnetic potentials on the nonlinear bending of PFGMTEEMs beams with simply supported ends

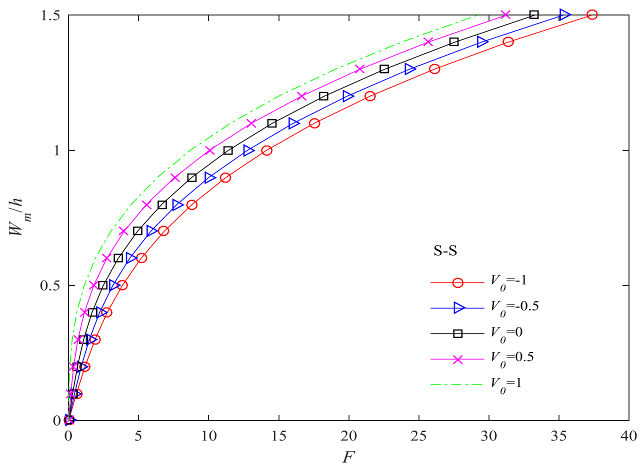

Fig. 17 The effect of external electric voltages on the nonlinear bending of PFGMTEEMs beams with simply supported ends

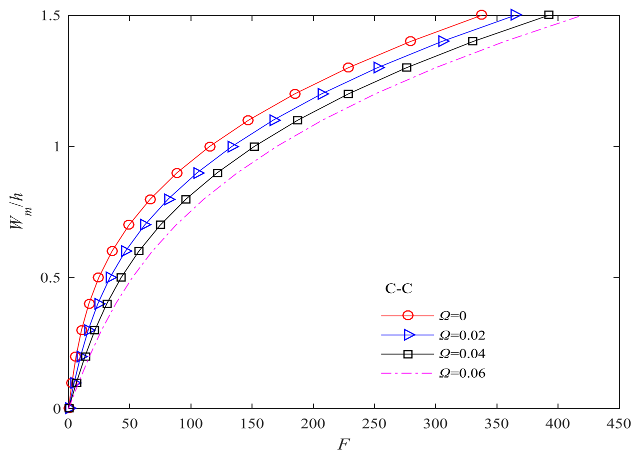

Fig. 20 The effect of initial magnetic potentials on the nonlinear bending of PFGMTEEMs beams with immovable clamped ends

The effect of initial magnetic potentials on the nonlinear bending of PFGMTEEMs beams under uniform transverse loading with simply supported ends and immovable clamped ends are shown in Figs. 19 and 20, where h = 20 nm, $b = h$, μ = 1 nm, l = 2 nm, L = 15 h, γ = 0.1, N = 1, T = 300 K, V_0 = 0 v. It can be found that if initial magnetic potentials are improved steadily, the deflection of beams is going to decrease prominently. The reason is that compared with the external electric voltage, initial magnetic potential has the opposite effect on the stiffness of beams due to compressive and tensile forces being produced via applying negative and positive magnetic potentials respectively.

6. Conclusions

In this article, nonlinear bending of functionally graded porous nanobeam subjected to multiple physical load is studied within the framework of nonlocal strain graded theory. Firstly, the displacement functions regarding the physical neutral surface in conjunction with the novel formulation of the effective material properties of porous beams are employed to derive the nonlinear bending governing equations of PFGMTEEMs beams, which are much more suitable to the actual porosity distribution and material distribution. Then, the corresponding analytical solutions are obtained by using an improved perturbation method. Finally, some significant conclusions can be drawn through conducting a detailed parametric analysis.

- The dimensionless deflection of beams becomes larger and larger with the increment of the content of BaTiO3.
- The overall stiffness of beams is reduced by the augment of porosity volume fraction, thereby resulting in the increment in the dimensionless deflection.
- The increase of strain gradient parameter l can improve the effective stiffness of beams.
- The nonlocal effect of static bending deformation is not only dependent on nonlocal parameter μ but also influenced by distributed transverse load, especially for a big transverse load.
- For linear and nonlinear bending obtained by nonlocal strain graded theory may be equal to ones obtained by classical elasticity theory and also may be smaller or bigger, which are dependent on nonlocal parameter, strain gradient parameter and the ratio of strain gradient parameter to nonlocal parameter.
- No matter which type of boundary conditions a beam is subjected to, the rise of dimensionless temperature and the increment of external electric voltages can increase the dimensionless deflection of beams, but the increment of initial magnetic potentials can decrease the dimensionless deflection of beams.

The above-obtained conclusions can provide theoretical references for optimization designs of structures made of FGMTEEMs under complicated conditions. Moreover, they are also immensely useful for others undertaking the analysis of porous nano-materials.

References

Abdelaziz, H.H., Meziane, M.A.A., Bousahla, A.A., Tounsi, A., Mahmoud, S.R. and Alwabli, A.S. (2017), "An efficient hyperbolic shear deformation theory for bending, buckling and free vibration of FGM sandwich plates with various boundary conditions", *Steel Compos. Struct., Int. J.*, **25**(6), 693-704. http://dx.doi.org/10.12989/scs.2017.25.6.693

Ansari, R., Hasrati, E., Gholami, R. and Sadeghi, F. (2015), "Nonlinear analysis of forced vibration of nonlocal third-order shear deformable beam model of magneto-electro-thermo elastic nanobeams", *Compos. Part B Eng.*, **83**, 226-241.

Arani, A.G., Maraghi, Z.K., Mozdianfard, M.R. and Shajari, A.R. (2010), "Thermo-piezo-magneto-mechanical stresses analysis of FGPM hollow rotating thin disk", *Int. J. Mech. Mater. Des.*, **6**(4), 341-349.

Attia, A., Tounsi, A., Adda Bedia, E.A. and Mahmoud, S.R. (2015), "Free vibration analysis of functionally graded plates with temperature-dependent properties using various four variable refined plate theories", *Steel Compos. Struct., Int. J.*, **18**(1), 187-212. http://dx.doi.org/10.12989/scs.2015.18.1.187

Barati, M.R. (2017), "On non-linear vibrations of flexoelectric nanobeams", *Int. J. Eng. Sci.*, 121, 143–153.

Bhattacharya, S. and Debabrata, D. (2019), "Free vibration analysis of bidirectional-functionally graded and double-tapered rotating micro-beam in thermal environment using modified couple stress theory", *Compos. Struct.*, **215**, 471-492.

Chen, D., Yang, J. and Kitipornchai, S. (2015), "Elastic buckling and static bending of shear deformable functionally graded porous beam", *Compos. Struct.*, **133**, 54-61.

Chen, D., Kitipornchai, S. and Yang, J. (2016), "Nonlinear free vibration of shear deformable sandwich beam with a functionally graded porous core", *Thin-Wall. Struct.*, **107**, 39-48.

Chen, X.C., Zhang, X.L., Lu, Y.X., et al. (2019), "Static and dynamic analysis of the postbuckling of bi-directional functionally graded material microbeams", *Int. J. Mech. Sci.*, **151**, 424-443.

Dai, T. and Dai, H.L. (2017), "Analysis of a rotating fgmee circular disk with variable thickness under thermal environment", *Appl. Math. Model*, **45**, 900-924.

Dai, H., Yue, X., Yuan, J. and Atluri, S.N. (2014), "A time domain collocation method for studying the aeroelasticity of a two dimensional airfoil with a structural nonlinearity", *J. Compos. Phys.*, **270**(3), 214-237.

Dehrouyeh-Semnani, A.M. (2017), "On boundary conditions for thermally loaded FG beams", *Int. J. Eng. Sci.*, **119**, 109-127.

Dehrouyeh-Semnani, A.M. (2018), "On the thermally induced non-linear response of functionally graded beams", *Int. J. Eng. Sci.*, **125**, 53-74.

Dehrouyeh-Semnani, A.M. and Bahrami, A. (2016), "On size-dependent Timoshenko beam element based on modified couple stress theory", *Int. J. Eng. Sci.*, **107**, 134-148.

Dehrouyeh-Semnani, A.M., Dehrouyeh, M., Torabi-Kafshgari, M. and Nikkhah-Bahrami, M. (2015), "An investigation into size-dependent vibration damping characteristics of functionally graded viscoelastically damped sandwich microbeams", *Int. J. Eng. Sci.*, **96**, 68-85.

Dehrouyeh-Semnani, A.M., Mostafaei, H. and Nikkhah, M., (2016), "Free flexural vibration of geometrically imperfect functionally graded microbeams", *Int. J. Eng. Sci.*, **105**, 56-79.

Dehrouyeh-Semnani, A.M., Mostafaei, H., Dehrouyeh, M. and Nikkhah-Bahrami, M. (2017), "Thermal pre- and post-snapthrough buckling of a geometrically imperfect doubly-clamped microbeam made of temperature-dependent functionally graded materials", *Compos. Struct.*, **170**, 122-134.

Ebrahimi, F. and Dabbagh, A. (2017a), "Nonlocal strain gradient based wave dispersion behavior of smart rotating magneto-electro-elastic nanoplates", *Mater Research Express*, **4**(2).

Ebrahimi, F. and Dabbagh, A. (2017b), "On flexural wave propagation responses of smart FG magneto-electro-elastic nanoplates via nonlocal strain gradient theory", *Compos. Struct.*, **162**, 281-293.

Ebrahimi, F. and Barati, M.R. (2016a), "Dynamic modeling of a thermo–piezo-electrically actuated nanosize beam subjected to a magnetic field", *Appl. Phys. A*, **122**(4), 1-18.

Ebrahimi, F. and Barati, M.R. (2016b), "A nonlocal higher-order shear deformation beam theory for vibration analysis of size-dependent functionally graded nanobeams", *Arab. J. Sci. Eng.*, **41**(5), 1-12.

Ebrahimi, F. and Barati, M.R. (2016c), "Through-the-length temperature distribution effects on thermal vibration analysis of nonlocal strain-gradient axially graded nanobeams subjected to nonuniform magnetic field", *J. Therm. Stress.*, **40**(5), 548-563.

Ebrahimi, F. and Barati, M.R. (2017), "Longitudinal varying elastic foundation effects on vibration behavior of axially graded nanobeams via nonlocal strain gradient elasticity theory", *Mech. Adv. Mater. Struct.*, **25**(11), 953-963.

El-Borgi, S., Rajendran, P., Friswell, M.I., Trabelssi, M. and Reddy, J.N. (2018), "Torsional vibration of size-dependent viscoelastic rods using nonlocal strain and velocity gradient theory", *Compos. Struct.*, **186**, 274-292.

Eltaher, M.A., Alshorbagy, A.E. and Mahmoud, F.F. (2013), "Determination of neutral axis position and its effect on natural frequencies of functionally graded macro/nanobeams", *Compos. Struct.*, **99**(5), 193-201.

Eringen, A.C. and Edelen, D.G.B. (1972), "On nonlocal elasticity", *Int. J. Eng. Sci.*, **10**(3), 233-248.

Esfahani, S.E., Kiani, Y. and Eslami, M.R. (2013), "Non-linear thermal stability analysis of temperature dependent FGM beams supported on non-linear hardening elastic foundations", *Int. J. Mech. Sci.*, **69**, 10-20.

Farajpour, A., Ghayesh, H.M. and Farokhi, H. (2018), "A review on the mechanics of nanostructures", *Int. J. Eng. Sci.*, **133**, 231-263.

Farajpour, A., Ghayesh, M.H, and Farokhi, H. (2019), "Large-amplitude coupled scale-dependent behaviour of geometrically imperfect NSGT nanotubes", *Int. J. Mech. Sci.*, **150**, 510-525.

Fourn, H., Atmane, H.A., Bourada, M., Bousahla, A.A., Tounsi, A. and Mahmoud, S.R. (2018), "A novel four variable refined plate theory for wave propagation in functionally graded material plates", *Steel Compos. Struct.*, *Int. J.*, **27**(1), 109-122. http://dx.doi.org/10.12989/scs.2018.27.1.109

Ghadiri, M., Rajabpour, A. and Akbarshahi, A. (2017), "Non-linear forced vibration analysis of nanobeams subjected to moving concentrated load resting on a viscoelastic foundation considering thermal and surface effects", *Appl. Math. Model.*, **50**, 676–694.

Ghayesh, M.H. and Farajpour, A. (2018a), "Nonlinear mechanics of nanoscale tubes via nonlocal strain gradient theory", *Int. J. Eng. Sci.*, **129**, 84-95.

Ghayesh, M.H. and Farajpour, A. (2018b), "Nonlinear coupled mechanics of nanotubes incorporating both nonlocal and strain gradient effects", *Mech. Adv. Mater. Struct.*, 1-10.

Ghayesh, M.H. and Farajpour, A. (2019), "A review on the mechanics of functionally graded nanoscale and microscale structures", *Int. J. Eng. Sci.*, **137**, 8-36.

Ghayesh, M.H., Farokhi, H. and Gholipour, A. (2017), "Resonance responses of geometrically imperfect functionally graded extensible microbeams", **12**(5), 051002.

Guo, J. and Wang, Y. (2017), "Size-dependent three-phase cylinder model of magnetoelectroelastic nanocomposites with interface effect under antiplane shear", *Acta Mech.*, **229**(3), 1-16.

Hall, K.C., Thomas, J.P. and Clark, W.S. (2015), "Computation of unsteady nonlinear flows in cascades using a harmonic balance technique", *Aiaa. J.*, **40**(5), 879-886.

Hamidi, A., Houari, M.S.A., Mahmoud, S.R. and Tounsi, A. (2015), "A sinusoidal plate theory with 5-unknowns and stretching effect for thermomechanical bending of functionally graded sandwich plates", *Steel Compos. Struct.*, *Int. J.*, **18**(1), 235-253. http://dx.doi.org/10.12989/scs.2015.18.1.235

Hao, F.Q. (2007), "Thermal post-buckling analyses of functionally graded material rod", *Appl. Math. Mech.*, **28**(1), 59-67.

Jha, D.K., Tarun, K. and Singh, R.K. (2013), "A critical review of recent research on functionally graded plates", *Compos. Struct.*, **96**(4), 833-849.

Ke, L.L., Wang, Y.S. and Wang, Z.D. (2012), "Nonlinear vibration of the piezoelectric nanobeams based on the nonlocal theory", *Compos. Struct.*, **94**(6), 2038-2047.

Kieback, B., Neubrand, A. and Riedel, H. (2003), "Processing techniques for functionally graded materials", *Mater. Sci. Eng. A*, **362**(1), 81-106.

Koizumi, M. (1997), "FGM activities in Japan", *Compos. Part B Eng.*, **28**(1-2), 1-4.

Lam, D.C., Yang, F., Chong, A.C.M., Wang, J. and Tong, P. (2003), "Experiments and theory in strain gradient elasticityz", *J. Mech. Phys. Solids*, **51**, 1477-1508.

Lei, J., He, Y., Guo, S., Li, Z. and Liu, D. (2016), "Size-dependent vibration of nickel cantilever microbeams: Experiment and gradient elasticity", *Aip Adv.*, **10**, 51-59.

Li, L., Li, X. and Hu, Y. (2016a), "Free vibration analysis of nonlocal strain gradient beams made of functionally graded material", *Int. J. Eng. Sci.*, **102**, 77-92.

Li, L., Hu, Y. and Li, X. (2016b), "Longitudinal vibration of size-dependent rods via nonlocal strain gradient theory", *Int. J. Mech. Sci.*, **115-116**, 135-144.

Li, X., Li, L., Hu, Y., Ding, Z. and Deng, W. (2017), "Bending, buckling and vibration of axially functionally graded beams based on nonlocal strain gradient theory", *Compos. Struct.*, **165**, 250-265.

Liebold, C. and Müller, W. (2016), "Comparison of gradient elasticity models for the bending of micromaterials", *Compos. Mater. Sci.*, **116**, 52-61.

Lim, C.W., Zhang, G. and Reddy, J.N. (2015), "A higher-order nonlocal elasticity and strain gradient theory and its applications in wave propagation", *J. Mech. Phys. Solids*, **78**, 298-313.

Liu, H., Lv, Z. and Wu, H. (2019), "Nonlinear free vibration of geometrically imperfect functionally graded sandwich nanobeams based on nonlocal strain gradient theory", *Compos. Struct.*, **214**, 47-61.

Lu, L., Guo, X. and Zhao, J. (2017), "Size-dependent vibration analysis of nanobeams based on the nonlocal strain gradient theory", *Int. J. Eng. Sci.*, **116**, 12-24.

Ma, L.S. and Lee, D.W. (2011), "A further discussion of nonlinear mechanical behavior for FGM beams under in-plane thermal loading", *Compos. Struct.*, **93**(2), 831-842.

Ma, L.H., Ke, L.L., Reddy, J.N., Yang, J., Kitipornchai, S. and Wang, Y.S. (2017), "Wave propagation characteristics in magneto-electro-elastic nanoshells using nonlocal strain gradient theory", *Compos. Struct.*, **199**, 10-20.

Menasria, A., Bouhadra, A., Tounsi, A., Bousahla, A.A. and Mahmoud, S.R. (2017), "A new and simple HSDT for thermal stability analysis of FG sandwich plates", *Steel Compos. Struct.*, *Int. J.*, **25**(2), 157-175. http://dx.doi.org/10.12989/scs.2017.25.2.157

Mindlin, R.D. (1965), "Second gradient of strain and surface-tension in linear elasticity", *Int. J. Solids Struct.*, **1**(4), 417-438.

Miyamoto, Y., Kaysser, W.A. and Rabin, B.H. (2001), "Functionally graded materials", *Encyclopedia Mater*, *Sci*. *Tech*., **44**(497), 3407-3413.

Mook, D. and Nayfeh, A. (1979), *Nonlinear Oscillations*, John Wiley & Sons, New York, NY, USA.

Nejad, M.Z., Hadi, A. and Rastgoo, A. (2016), "Buckling analysis of arbitrary two-directional functionally graded euler-bernoulli nano-beams based on nonlocal elasticity theory", *Int*. *J*. *Eng*. *Sci*., **103**, 1-10.

Rahmani, O. and Pedram, O. (2014), "Analysis and modeling the size effect on vibration of functionally graded nanobeams based on nonlocal timoshenko beam theory", *Int*. *J*. *Eng*. *Sci*., **77**(7), 55-70.

Saadatfar, M. and Aghaie-Khafri, M. (2014), "Hygrothermo-magnetoelectroelastic analysis of a functionally graded magnetoelectroelastic hollow sphere resting on an elastic foundation", *Smart Mater*. *Struct*., **23**(3), 35004-35016.

Sahmani, S., Aghdam, M.M. and Rabczuk, T. (2018), "Nonlocal strain gradient plate model for nonlinear large-amplitude vibrations of functionally graded porous micro/nano-plates reinforced with gpls", *Compos*. *Struct*., **198**, 51-62.

She, G.L., Yuan, F.G., Ren, Y.R. and Xiao, W.S. (2017), "On buckling and postbuckling behavior of nanotubes", *Int*. *J*. *Eng*. *Sci*., **121**, 130-142.

She, G.L., Ren, Y.R., Yuan, F.G. and Xiao, W.S. (2018a), "On vibrations of porous nanotubes", *Int*. *J*. *Eng*. *Sci*., **125**, 23-35.

She, G.L., Yuan, F.G. and Ren, Y.R. (2018b), "On wave propagation of porous nanotubes", *Int*. *J*. *Eng*. *Sci*., **130**, 62-74.

She, G.L., Yan, K.M., Zhang, Y.L., Liu, H.B. and Ren, Y.R. (2018c), "Wave propagation of functionally graded porous nanobeams based on non-local strain gradient theory", *Eur*. *Phys*. *J*. *Plus*, **133**(9), p. 368.

She, G.L., Yuan, F.G., Ren, Y.R., Liu, H.B. and Xiao, W.S. (2018d), "Nonlinear bending and vibration analysis of functionally graded porous tubes via a nonlocal strain gradient theory", *Compos*. *Struct*., **203**, 614-623.

She, G.L., Yuan, F.G., Karami, B., Ren, Y.R. and Xiao, W.S. (2019), "On nonlinear bending behavior of FG porous curved nanotubes", *Int*. *J*. *Eng*. *Sci*., **135**, 58-74.

Şimşek, M. (2016), "Nonlinear free vibration of a functionally graded nanobeam using nonlocal strain gradient theory and a novel hamiltonian approach", *Int*. *J*. *Eng*. *Sci*., **105**, 12-27.

Simsek, M. and Reddy, J.N. (2013), "Bending and vibration of functionally graded microbeams using a new higher order beam theory and the modified couple stress theory", *Int*. *J*. *Eng*. *Sci*., **64**(1), 37-53.

Tang, C. and Alici, G. (2011a), "Evaluation of length-scale effects for mechanical behaviour of micro- and nanocantilevers: I. Experimental determination of length-scale factors", *J*. *Phys*. *D*. *Appl*. *Phys*., **44**(33), 335501.

Tang, C. and Alici, G. (2011b), "Evaluation of length-scale effects for mechanical behaviour of micro- and nanocantilevers: II. Experimental verification of deflection models using atomic force microscopy", *J*. *Phys*. *D*. *Appl*. *Phys*., **44**(33), 335502.

Tao, M.A., Zhao, Z.M., Liu, L.X., Gao, C. and Huang, X.G. (2012), "The research development and future application of functionally gradient materials", *Sci*. *Tech*. *Chem*. *Ind*.

Thai, S., Thai, H.T., Vo, T.P. and Patel, V.I. (2018), "A simple shear deformation theory for nonlocal beams", *Compo*. *Struct*., **1**, 262-270.

Trinh, L.C., Nguyen, H.X., Vo, T.P. and Nguyen, T.K (2016), "Size-dependent behaviour of functionally graded microbeams using various shear deformation theories based on the modified couple stress theory", *Compos*. *Struct*., **154**, 556-572.

Wu, H.L., Kitipornchai, S. and Yang, J. (2016), "Thermal Buckling and Postbuckling Analysis of Functionally Graded Carbon Nanotube-Reinforced Composite Beams", *Appl*. *Mech*., *Mater*., **846**, 182-187.

Xiao, W.S., Gao, Y. and Zhu, H.P. (2018), "Buckling and post-buckling of magneto-electro-thermo-elastic functionally graded porous nanobeams", *Microsyst*. *Technol*. https://doi.org/10.1007/s00542-018-4145-2

Yang, F.A.C.M., Chong, A.C.M., Lam, D.C.C. and Tong, P. (2002), "Couple stress based strain gradient theory for elasticity", *Int*. *J*. *Solids Struct*., **39**, 2731-2743.

Zhang, D.G. (2013), "Nonlinear bending analysis of fgm beams based on physical neutral surface and high order shear deformation theory," *Compos*. *Struct*., **100**(5), 121-126.

Zhang, D.G. (2015), "Nonlinear static analysis of fgm infinite cylindrical shallow shells based on physical neutral surface and high order shear deformation theory", *Appl*. *Math*. *Model*., **39**(5-6), 1587-1596.

Zhang, P. and Fu, Y. (2013), "A higher-order beam model for tubes", *Eur. J. Mech. A Solids*, **38**, 12-19.

Zhang, D.G. and Zhou, Y.H. (2009), "A theoretical analysis of fgm thin plates based on physical neutral surface", *Compos*. *Mater*. *Sci*., **44**(2), 716-720.

Zhong, J., Fu, Y., Wan, D. and Li, Y. (2016), "Nonlinear bending and vibration of functionally graded tubes resting on elastic foundations in thermal environment based on a refined beam model", *Appl*. *Math*. *Model*., **40**(17-18), 7601-7614.

Zhou, J. (1986), *Differential Transformation and its Applications for Electrical Circuits*, Huazhong University Press, Wuhan, China.

CC